

Mitochondria affect photosynthesis through altered tissue levels of O₂

Matleena Punkkinen¹, Bikash Baral¹, Olga Blokhina^{1#}, Lucas León Peralta Ogorek^{2,3#}, Minsoo Kim^{4#§}, Kurt Fagerstedt¹, Mikael Brosché¹, Lauri Nikkanen⁵, Elizabeth Vierling⁴, Ole Pedersen², Alexey Shapiguzov^{1,6*}

1. Organismal and Evolutionary Biology (OEB), Viikki Plant Science Centre (ViPS), Faculty of Biological and Environmental Sciences, University of Helsinki, Helsinki 00014, Finland.
2. Freshwater Biological Laboratory, Department of Biology, University of Copenhagen, Copenhagen 2100, Denmark.
3. School of Biosciences, University of Nottingham, Sutton Bonington LE12 5RD, United Kingdom.
4. Department of Biochemistry & Molecular Biology, University of Massachusetts Amherst, Amherst MA 01003, USA.
5. Molecular Plant Biology, Department of Life Technologies, University of Turku, Turku 20014, Finland.
6. Natural Resources Institute Finland (Luke), Production Systems, Turku 20520, Finland.

These authors contributed equally to the manuscript

§Current address: Howard Hughes Medical Institute and Department of Molecular Biology, Massachusetts General Hospital, Boston MA 02114, USA.

* Corresponding author: Alexey Shapiguzov (alexey.shapiguzov@helsinki.fi)

The author responsible for distribution of materials integral to the findings presented in this article in accordance with the policy described in the Instructions for Authors (<https://academic.oup.com/plphys/pages/General-Instructions>) is Alexey Shapiguzov.

Short title: Mitochondrial O₂ consumption alters photosynthesis

Abstract

Oxygen (O₂) availability in plant tissues is dynamically shaped by photosynthesis and respiration and is linked to plant stress responses and development. While mitochondria are the primary consumers of cellular O₂, their impact on chloroplast functions under low-oxygen conditions remains insufficiently understood. Mitochondrial retrograde signaling activates expression of nuclear genes encoding alternative oxidases and other respiratory components, and high abundance of these enzymes coincides not only with changes in respiration but also with alterations in chloroplast functions. For example, plants with induced mitochondrial signaling are tolerant to methyl viologen, which catalyzes the Mehler reaction. The mechanism of this inter-organelle interaction remains unclear. Here, we investigated respiration,

© The Author(s) 2025. Published by Oxford University Press on behalf of American Society of Plant Biologists. This is an Open Access article distributed under the terms of the Creative Commons Attribution License (<https://creativecommons.org/licenses/by/4.0/>), which permits unrestricted reuse, distribution, and reproduction in any medium, provided the original work is properly cited.

1 photosynthesis, and *in vivo* O₂ levels in Arabidopsis (*Arabidopsis thaliana*) mutants and
2 transgenic lines with perturbations in diverse mitochondrial functions, including defects in
3 respiratory complex I, ATP synthase, mitochondrial protein processing, transcription, nucleoid
4 organization, and organelle architecture; as well as in lines with altered mitochondrial
5 signaling, alternative oxidase activities, and nitric oxide metabolism. Increased abundance and
6 capacity of alternative oxidases correlated with elevated O₂ consumption in darkness, slower
7 O₂ re-accumulation in light, and reduced effects of methyl viologen on chloroplasts. The
8 changes are likely mediated by multiple stress-induced alternative respiratory components. Our
9 results support the hypothesis that enhanced mitochondrial O₂ consumption under stress lowers
10 tissue O₂ levels, thereby modifying chloroplastic electron transfer and ROS metabolism. These
11 data provide insights into the establishment and sensing of hypoxia in plants, plant adaptation
12 to mitochondrial stress and low-oxygen environments, and the roles of chloroplasts in these
13 processes.

15 Introduction

16 Cellular consumption, production, and sensing of molecular oxygen (O₂) are tightly integrated
17 with plant metabolic and signaling networks (Bailey-Serres et al., 2024; Van Veen et al., 2025,
18 Renziehausen et al., 2024). Oxygen availability in plant tissues fluctuates over diurnal cycles,
19 influenced by both photosynthesis and respiration (Triozi et al., 2024). Localized hypoxia,
20 which can be caused by elevated mitochondrial respiration, has been implicated in stress
21 acclimation (Wang et al., 2020) and developmental regulation (Weits et al., 2021; Iida et al.,
22 2025). These observations highlight a link between low-oxygen signaling and energy
23 metabolism.

24 Mitochondria are the main consumers of cellular O₂. In these organelles, O₂ acts as the terminal
25 electron acceptor for respiration in the cytochrome *c* oxidase (COX) and alternative oxidase
26 (AOX) pathways. AOXs, together with alternative NAD(P)H dehydrogenases (NDs), form a
27 stress-inducible, non-phosphorylating electron transfer system that dissipates excessive
28 reducing power (Yoshida and Noguchi, 2011; Vanlerberghe, 2013; Wagner et al., 2018;
29 Shameer et al., 2019; Møller et al., 2021). The alternative respiratory pathway is often induced
30 under stress and is associated with mitochondrial retrograde signaling, which activates a set of
31 nuclear genes referred to as the mitochondrial dysfunction stimulon (MDS) (De Clercq et al.,
32 2013; Ng et al., 2013; Shapiguzov et al., 2019; Eysholdt-Derzsó et al., 2023; Khan et al., 2024).
33 MDS signaling plays an important role in the adaptation of plants to low-oxygen levels
34 (Renziehausen et al., 2024).

1 While the roles of mitochondria under changing tissue O₂ levels are well established, how
2 chloroplast functions integrate into this network remains less clear. Inside the chloroplast, O₂ is
3 produced by light-driven water splitting and consumed by photorespiration (Bauwe et al.,
4 2010), the plastid terminal oxidase (PTOX) (Nawrocki et al., 2015), and the Mehler reaction
5 (Miyake et al., 2010). In the Mehler reaction, electrons are transferred from Photosystem I
6 (PSI) to O₂, generating reactive oxygen species (ROS). Interestingly, ROS metabolism of the
7 chloroplast is sensitive to mitochondrial MDS signaling: plants with activated MDS exhibit
8 tolerance to methyl viologen (MV, also known as paraquat) (De Clercq et al., 2013; Ng et al.,
9 2013; Shapiguzov et al., 2019), a catalyst of the Mehler reaction. Treatment with MV generates
10 ROS that can overwhelm the chloroplast antioxidant systems, resulting in photoinhibition and
11 cell death (Farrington et al., 1973; Nishiyama et al., 2011; Shapiguzov et al., 2019). Another
12 phenotype associated with MDS activation is a more reduced redox state of chloroplast thiol
13 enzymes (Shapiguzov et al., 2019; Shapiguzov et al., 2020). This is consistent with attenuation
14 of the Mehler reaction, as Mehler-derived ROS are the main oxidants of these enzymes (Ojeda
15 et al., 2018; Vaseghi et al., 2018; Yoshida et al., 2018).

16 We previously proposed that elevated mitochondrial respiration in plants with active MDS
17 reduces O₂ availability, thereby modifying ROS metabolism of the chloroplast (Shapiguzov et
18 al., 2020). However, direct evidence for altered O₂ levels has been lacking. In this study we
19 investigated photosynthesis, respiration and *in vivo* O₂ levels in a set of Arabidopsis
20 (*Arabidopsis thaliana*) mutants and transgenic lines with defects in diverse mitochondrial
21 functions (Fig. 1), including respiratory complex I (*ndufa1*, *ndufs4*, *rug3*), ATP synthase (*ATPd*
22 RNAi line here called *ATPQi*), protein processing (*phb3*, *lon1*), transcription and nucleoid
23 organization (*rpoTmp*, *shot1*, *atad3a1 atad3b1:ATAD3A1-GFP* here called *ATAD3A1-GFP*),
24 and architecture and fission (*drp3a drp3b*, *mic60*). Additionally, we examined mutants and
25 transgenic lines with altered MDS signaling and AOX activities (*rcd1*, *rcd1 anac017*,
26 *ANAC013* overexpressor line *ANAC013-OE*, *aox1a*, *aox1a aox1d*, *AOX1a* overexpressor line
27 here called *AOX1a-OE*), or altered nitric oxide (NO) metabolism (*hot5*, and a *GSNOR*
28 overexpressor line *GSNOR-GFP*).

29 Our results support the hypothesis that enhanced mitochondrial O₂ consumption under stress
30 conditions contributes to lower tissue levels of O₂, which in turn affects chloroplast functions
31 and photosynthesis. These data provide insights into the establishment and sensing of hypoxia

1 in plants, plant adaptation to mitochondrial stress and low-oxygen environments, and the roles
2 of chloroplasts in these processes.

4 **Results**

5 *Mitochondrial perturbations modify plants' responses to MV*

6 Mitochondrial defects associated with increased MDS signaling coincide with changes in the
7 chloroplasts (De Clercq et al., 2013; Ng et al., 2013; Shapiguzov et al., 2019; Shapiguzov et al.,
8 2020). To test whether this is a general response to various mitochondrial perturbations, rather
9 than a consequence of specific mitochondrial defects, we studied reactions to MV in a set of
10 Arabidopsis mutants and transgenic lines with impaired mitochondrial functions (Fig. 1). We
11 began by assessing the tolerance of these lines to MV-induced photoinhibition, an indication of
12 damage to photosynthetic apparatus due to ROS. Leaf discs were floated overnight in darkness
13 on solutions with or without MV to facilitate uptake of the chemical. After incubation, MV
14 toxicity was induced by 15 repeated 1-hour light periods (450 nm, 80 $\mu\text{mol m}^{-2} \text{s}^{-1}$) each
15 followed by a 20-min dark acclimation period and a measurement of maximal quantum yield of
16 Photosystem II (PSII) (Fv/Fm). No significant changes were observed in either Fv/Fm or leaf
17 AOX abundance during the overnight incubation of leaf discs (Supplementary Figure 1 A, B).
18 After the overnight incubation but before the start of the light exposure Fv/Fm was in the range
19 of 0.8-0.85 in both MV-treated and control samples of all tested genotypes (Supplementary
20 Figure 1C). This indicated that the assessed effects of MV were light-dependent and thus likely
21 caused by MV action in the chloroplast. Several plant lines that are affected in different
22 mitochondrial processes were more tolerant to MV, maintaining relatively stable Fv/Fm values
23 during 15 hours of light treatment, in comparison to the wild type (Col-0) that showed a
24 dramatic reduction in PSII quantum yield (Fig. 2A). A comparison of end point Fv/Fm values
25 for all lines (Fig. 2B) shows that over half of the tested genotypes that are deficient in diverse
26 mitochondrial functions exhibit resistance to chloroplastic ROS stress.

27
28 In addition to its long-term effects on chloroplasts and the photosynthetic apparatus associated
29 with ROS production, MV also induces rapid changes in the redox state of the photosynthetic
30 electron transfer chain. These changes are detectable already within one second of light

1 exposure (Shapiguzov et al., 2020). The effect is likely caused by MV acting as a strong
2 electron sink at the electron-acceptor side of PSI, withdrawing electrons from the FeS clusters
3 (Tiwari et al., 2024). This promotes oxidation of the photosynthetic electron transfer chain and
4 thus faster quenching of chlorophyll fluorescence. We previously showed that in a normoxic
5 atmosphere (normal air) the quenching effect that MV has on chlorophyll fluorescence is
6 indistinguishable between the wild type and *rcd1*. However, under hypoxia MV-induced
7 chlorophyll fluorescence quenching diminished in *rcd1* while remaining high in the wild type
8 (Shapiguzov et al., 2020). We therefore tested the effects of MV under an hypoxic atmosphere
9 in all lines. We floated leaf discs overnight on solutions with or without MV in darkness under
10 ambient atmosphere. Next, we introduced an hypoxic environment by flushing nitrogen gas
11 over the leaf discs for 20 min in darkness, and finally, we performed light treatments and
12 recorded the chlorophyll fluorescence responses.

13 First, we measured the rapid (within 50 sec) dark relaxation of maximal chlorophyll
14 fluorescence (F_m) triggered by a saturating light pulse (Fig. 2C, D), then the dynamics of
15 chlorophyll fluorescence under low-intensity actinic light (Fig. 2E, F). In both types of
16 measurements, chlorophyll fluorescence responses were similar in all lines under a normoxic
17 environment (Supplementary Figure 2A, B; Supplementary Dataset S1) and under hypoxic
18 atmosphere without MV (Supplementary Figure 2C; Supplementary Dataset S1). However,
19 under hypoxic conditions the effect of MV on fluorescence quenching was strikingly different
20 between the genotypes (Fig. 2C-F; Supplementary Dataset S1). In wild-type plants, MV still
21 efficiently quenched chlorophyll fluorescence, while in several lines with impaired
22 mitochondria, fluorescence dynamics of MV-treated samples became indistinguishable from
23 untreated controls (compare Fig. 2E and Supplementary Figure 2C). These results indicate that
24 O_2 availability is crucial for mitochondrial modulation of the measured chloroplast functions.

25 The main known pathways through which O_2 affects chloroplastic electron flows are the
26 Mehler reaction at the PSI acceptor side, the activity of the chloroplast terminal oxidase PTOX,
27 and photorespiration. PTOX was previously not implicated in MV tolerance (Shapiguzov et al.,
28 2019). To test whether the observed toxicity of MV is linked to photorespiration, we first
29 studied the responses of several plant lines to MV-induced photoinhibition under elevated CO_2
30 concentration (~1000 ppm), which suppresses photorespiration, versus normal atmospheric
31 CO_2 (~450 ppm). The F_v/F_m dynamics were very similar under both conditions in the studied

1 lines (Supplementary Figure 3). Next, we performed MV-induced photoinhibition analyses in
2 mutants deficient in photorespiration: *cat2* (lacking peroxisomal catalase 2), *gox1* (lacking
3 glycolate oxidase 1), *cat2 gox1*, and *rcd1 cat2*. Of these mutants, *cat2*, *gox1* and *cat2 gox1*
4 responded to MV in a similar manner to wild type, while *rcd1 cat2* performed similarly to *rcd1*
5 (Supplementary Figure 4). These results indicate that photorespiration does not substantially
6 contribute to the observed interaction between the organelles, thereby narrowing our focus to
7 the Mehler reaction.

8 The above experiments showed that various mitochondrial perturbations suppressed the effects
9 of MV on chloroplasts, indicating altered ROS metabolism and photosynthetic electron
10 transfer, and that this organelle interaction is sensitive to O₂ availability.

11 ***Mitochondria influence the Mehler reaction at PSI in an oxygen-dependent manner***

12 To probe the activity of MV at its site of action on the electron-acceptor side of PSI, we
13 measured the oxidation state of PSI reaction center P700 using DUAL-PAM. Detached leaves
14 were pretreated with 1 μM MV and placed in transparent bags with or without an AnaeroGen
15 anaerobic gas generator, after which light treatments and spectroscopic measurements were
16 performed through the plastic. Far red light (720 nm), preferentially absorbed by PSI, was
17 turned on to oxidize P700. Next, a saturating red light flash (635 nm), preferentially absorbed
18 by PSII, was turned on to transiently reduce P700 in the far red light background. As expected,
19 the reoxidation rate of P700 was strongly enhanced by MV in normoxic controls (Fig. 3A). In
20 leaves under hypoxic conditions, MV still accelerated PSI oxidation in Col-0, but not in *rcd1* or
21 *ATAD3A1-GFP* (Fig. 3A, B). Importantly, immunoblotting of these lines with the αPsaA
22 antibody revealed no difference in PSI abundance (Fig. 3C).

23 As a complementary approach, we performed flash-induced chlorophyll fluorescence imaging,
24 similarly to the measurements in Shapiguzov et al., 2020. The polyphasic rise of chlorophyll
25 fluorescence triggered by a saturating light pulse, the OJIP transient, reflects electron transfer
26 dynamics through different parts of the photosynthetic electron transfer chain. The O-J phase
27 corresponds to PSII, the J-I phase to the intersystem electron transfer chain, and the I-P rise to
28 PSI activity (Strasser et al., 2004; Stirbet and Govindjee, 2011; Stirbet and Govindjee, 2012;
29 Schreiber and Klughammer, 2021; Schreiber, 2023). MV application specifically diminished
30 the I-P rise, indicating oxidation of PSI in all tested lines (Supplementary Figure 5). However,

1 following 60 min of nitrogen flushing in darkness to induce hypoxia, the extent of the I–P rise
2 varied among the lines (Fig. 3D). We calculated $\phi_{RE10} = 1 - F_i/F_m$, a parameter sensitive to
3 MV effects on the I–P rise (Strasser et al., 2004; Shapiguzov et al., 2020), for MV-treated
4 samples and their controls. MV continued to suppress the I–P rise in the wild type, but its effect
5 was significantly diminished in several lines with impaired mitochondria (Fig. 3E;
6 Supplementary Dataset S1).

7 Together, these analyses demonstrated that the redox effects of MV on photosynthetic electron
8 transfer, and specifically on PSI, are modified in lines with altered mitochondrial functions.
9 Notably, these differences only became apparent under hypoxic conditions. This suggests that
10 the interaction between altered mitochondrial functions and PSI is dependent on O₂ availability.

12 ***Mitochondrial defects modify O₂ consumption and accumulation rates in vivo***

13 Observing that the effects of MV on chloroplasts were modulated by an externally generated
14 hypoxic atmosphere prompted us to study whether altered responses of mitochondrial mutants
15 to MV were linked to tissue O₂ levels. We hypothesized that the changes in respiration caused
16 by mitochondrial defects could affect tissue O₂ availability, thereby modulating the effects of
17 MV. Thus, we selected a subset of lines with the strongest changes in MV response compared
18 to the wild type and measured their rates of O₂ consumption in darkness and O₂ re-
19 accumulation in light. An example of such an assay is shown in Fig. 4A. We found several
20 lines that had higher O₂ consumption rates in darkness or lower O₂ re-accumulation rates in
21 light than in the wild type (Fig. 4B, C). Since studies in *rcd1* showed no defects in the
22 chloroplast proteome (Shapiguzov et al., 2019) or O₂ evolution (Shapiguzov et al., 2020), the
23 changes in O₂ re-accumulation rate were likely due to increased reuptake of photosynthetically
24 evolved O₂ instead of decreased O₂ evolution.

25 Next, we performed a similar experiment in the presence of the AOX inhibitor
26 salicylhydroxamic acid (SHAM). SHAM reduced the above differences between the lines
27 (Supplementary Figure 6), which suggests that the differences in O₂ dynamics could be related
28 to different levels of AOX activity.

29 In the above assays we measured exogenous levels of O₂ that diffused from plant tissues to the
30 media in the measurement cuvette. To determine whether we could also observe changed levels

1 of O₂ inside plant tissues, we examined the O₂ status inside the central veins of leaf blades *in*
2 *situ* using O₂ microsensors (Supplementary Figure 7A). Even though no statistical difference
3 was detected in O₂ consumption rates between Col-0 and *rcd1*, O₂ re-accumulation after the
4 start of illumination was suppressed in *rcd1* (Supplementary Figure 7B). This was in line with
5 the measurements of external O₂ dynamics in seedlings.

6 Overall, the results indicated altered tissue O₂ levels and changes in the O₂-dependent
7 chloroplastic processes in plant lines with deficient mitochondrial respiration, supporting the
8 role of intracellular O₂ exchange in the studied organelle interaction.

9 ***Diverse mitochondrial defects increase abundance and respiration capacity of AOXs***

10 A prominent feature of mitochondrial stress and the associated MDS transcriptional
11 reprogramming is the induction of AOXs, enzymes that have been implicated in the regulation
12 of cellular O₂ status. To evaluate the possible role of these enzymes in interregulation between
13 mitochondria and chloroplasts, we quantified AOX protein abundance across the plant lines by
14 immunoblotting with an antibody that recognizes all five Arabidopsis AOX isoforms
15 (α AOX1/2, Supplementary Figure 8A). The antibody showed linear response in the range of
16 1.75-70 μ g of total protein, making it suitable for the quantitative comparison of plant lines
17 with diverse AOX abundance (Supplementary Figure 8B). For most lines, differences in AOX
18 abundance remained consistent between the seedling and mature growth stages (Supplementary
19 Figure 8C). Several of the tested plant lines with mitochondrial defects demonstrated a
20 statistically significant increase in AOX abundance compared to the wild type (Fig. 5A). For
21 example, in *rcd1* AOX abundance was 8.7 ± 3.5 times higher and in *ndufs4* it was 7.8 ± 2.5
22 times higher than in Col-0 (Fig. 5A and Supplementary Dataset S1). We additionally assessed
23 AOX respiration capacity by measuring changes in O₂ concentration in darkness in the
24 presence of KCN, the inhibitor of COX respiration. AOX activity is resistant to KCN; hence,
25 residual O₂ uptake in KCN-treated seedlings can be ascribed to AOXs. In several lines,
26 application of KCN led to only minor drops in O₂ consumption, indicating strong involvement
27 of AOX respiration in the overall O₂ uptake by the seedlings (Fig. 5B and Supplementary
28 Figure 8D). For example, in Col-0, *rcd1* and *ndufs4* KCN inhibited the O₂ consumption rate by
29 $83 \pm 15\%$, $17 \pm 9\%$ and $42 \pm 28\%$, respectively (Supplementary Figure 8D and Supplementary
30 Dataset S1). For all tested lines we found a correlation between AOX abundance and AOX

1 capacity (Pearson correlation from averages 0.8704, p-value < 0.0001) (Fig. 5C). These results
2 indicated that modified AOX respiration is a general response to diverse mitochondrial defects.

4 ***Roles of individual alternative respiratory enzymes in the organelle interaction***

5 Taken together, the results suggested a link between AOX abundance, AOX respiration
6 capacity, and various MV-related phenotypes. This connection could also be seen in a
7 correlation analysis, where AOX abundance correlated with AOX respiration capacity, while
8 all the described MV-related phenotypes correlated with each other (Fig. 6A), with the *AOX1a*-
9 OE line being one notable exception (Supplementary Figure 9A). When this plant line was
10 removed from the correlation analyses, a positive correlation was observed between AOX
11 abundance, AOX capacity and diverse MV phenotypes (Fig. 6A). Furthermore, resistance to
12 MV-induced photoinhibition showed a positive correlation with O₂ consumption rate in
13 darkness (Fig. 6A, B), and MV-related phenotypes also negatively correlated with O₂ re-
14 accumulation rate in light, although with low statistical significance. Interestingly, in MV
15 assays the *AOX1a*-OE line performed similarly to the wild type, suggesting that enhanced
16 expression of a single AOX1a isoform was not sufficient for the studied organellar interaction.

17 In *Arabidopsis thaliana* the repertoire of alternative respiratory enzymes includes five AOX
18 isoforms (AOX1a, -1b, -1c, -1d and -2) and six NDs (NDA1, -2; NDB1, -2, -3, 4; NDC1)
19 (Møller et al., 2021). AOX1a and AOX1d are the main stress-inducible AOX isoforms in
20 *Arabidopsis* leaves (Oh et al., 2022). To further assess their roles in the impact of respiration on
21 chloroplasts, we generated an *aox1a aox1d* double mutant, which showed similar AOX
22 capacity and MV-induced photoinhibition to Col-0 (Supplementary Figure 8D and
23 Supplementary Figure 9B, respectively). Notably, immunoblotting with α AOX1/2 antibody
24 still displayed another AOX isoform in *aox1a aox1d* (Supplementary Figure 9C). Thus, the
25 studied effects of mitochondrial respiration on chloroplasts could not be linked to specific AOX
26 isoform(s).

27 This result prompted us to examine whether other alternative respiratory enzymes contribute to
28 the inter-organelle interaction. We quantified their gene expression using publicly available
29 RNA transcriptome datasets for *gsnor1*, *lon1*, *mtran1 mtran2*, *phb3*, *rcd1* (two independent
30 datasets), and *rpoTmp*. Importantly, all the datasets showed increased expression of marker

1 genes for induced MDS signaling: *UPOX* (AT2G21640) and *HRG2* (AT5G24640).
2 Furthermore, in all datasets except *gsnor1* we observed increased expression of hypoxia
3 marker genes *ERF71* (AT2G47520), *HRU1* (AT3G03270) and *PDC1* (AT4G33070), with the
4 strongest increase in *ERF71*. Almost all genes encoding AOXs and NDs (*NDC1* being the
5 exception) showed significantly increased expression in at least one of the genetic
6 perturbations (Fig. 6C). These transcriptomic results indicate that mitochondrial dysfunction
7 triggers changes in the expression of not just *AOXs*, but a repertoire of alternative respiratory
8 enzymes.

9 Taken together, these results suggest a link between stress-induced changes in mitochondrial
10 respiration, tissue O₂ status, and the MV-catalyzed Mehler reaction. The contribution of
11 individual mitochondrial respiratory components in this inter-organelle interaction remains to
12 be refined.

14 Discussion

15 *The emerging interaction of plant mitochondria and chloroplasts through intracellular O₂* 16 *exchange*

17 We explored a link between mitochondrial respiration, altered tissue O₂ levels, and
18 chloroplastic functions, particularly as related to ROS metabolism. Evidence for such
19 interaction has accumulated across multiple studies. For example, hypoxic signaling influences
20 transcriptional control of chlorophyll biosynthesis (Abbas et al., 2022), mitochondrial
21 alternative respiratory components support photosynthetic activity (Jethva et al., 2022;
22 Renziehausen et al., 2024), and chloroplastic ROS homeostasis is modified by the MDS
23 pathway (De Clercq et al., 2013; Ng et al., 2013; Shapiguzov et al., 2019; Shapiguzov et al.,
24 2020). These observations indicate that chloroplasts actively partner with mitochondria in
25 responses to changing O₂ levels, yet the mechanistic connections remain poorly understood.
26 Analyses of plant lines with activated mitochondrial MDS signaling have not revealed
27 structural changes in chloroplasts that could explain modified chloroplastic functions (Jaspers
28 et al., 2009; Brosché et al., 2014; Shapiguzov et al., 2019). This suggests that mitochondria
29 influence chloroplasts through operational changes, such as altered metabolic fluxes, redox
30 shuttles, or gas exchange (Shapiguzov et al., 2019; Shapiguzov et al., 2020; Sipari et al., 2020).

1 Most studies have linked the effects of altered mitochondrial respiration on photosynthesis to
2 electron sink activities of AOXs. By consuming reducing equivalents from mitochondria and,
3 via redox shuttles, from chloroplasts, AOXs can limit ROS production in both organelles
4 (Yoshida and Noguchi, 2011; Vanlerberghe, 2013; Vanlerberghe et al., 2020; Bailleul et al.,
5 2015; Dahal and Vanlerberghe, 2017; Murik et al., 2019; Møller et al., 2021; Oh et al., 2022).
6 An inter-organelle electron transfer pathway, possibly involving a malate shuttle, was
7 proposed to compete with the Mehler reaction at the PSI acceptor side in the *rcd1* mutant,
8 which exhibits constitutive MDS activation and increased AOX abundance (Shapiguzov et al.,
9 2019).

10 A complementary explanation for how mitochondria influence ROS metabolism, including
11 ROS in the chloroplast, involves the oxygen-consuming activities of these organelles. This role
12 of mitochondria has been linked to diurnal changes in O₂ availability in young Arabidopsis
13 leaves (Triozzi et al., 2024), as well as to hypoxic niches in specialized tissues (Gupta et al.,
14 2009; Rasmusson et al., 2009; Kelliher and Walbot, 2012; Van Dongen and Licausi, 2015;
15 Gupta et al., 2018; Weits et al., 2021; Iida et al., 2025). Studies in photosynthetic tissues are
16 limited by technical challenges, as O₂ evolution during photosynthesis masks mitochondrial O₂
17 consumption in the light. To overcome this, we used two conditions that allowed us to observe
18 this interaction: hypoxia and treatment with MV, a catalyst of the Mehler reaction. MV
19 suppresses photosynthetic O₂ evolution, likely by perturbing redox regulation of the
20 chloroplastic ATP synthase (Nikkanen et al., 2024), which enhances thylakoid lumen
21 acidification, increases non-photochemical quenching, and thus inhibits PSII activity.
22 Importantly, MV does not inhibit CO₂ evolution, suggesting that mitochondrial respiration
23 remains active (Shapiguzov et al., 2020). These features create similarities between MV stress
24 and hypoxia and make MV a useful tool for this study. By catalyzing the Mehler reaction, MV
25 alters the PSI redox state and quenches chlorophyll fluorescence, providing measurable *in vivo*
26 signals that were instrumental for this study (Figs 2, 3).

27 Our results support the hypothesis that increased mitochondrial respiration, potentially
28 associated with enhanced AOX activity, modulates chloroplast functions by lowering
29 intracellular O₂. The effect of altered mitochondrial respiration on O₂-dependent and MV-
30 catalyzed PSI oxidation was observed as early as 20 min after exposure to exogenous hypoxia

1 (Fig. 2C-F), suggesting that in addition to possible de novo transcriptional reprogramming
2 induced by hypoxic treatment, pre-existing metabolic changes caused by altered mitochondrial
3 functions play a central role. A plausible explanation for these observations is that O₂ limitation
4 caused by enhanced respiration suppressed the Mehler reaction at PSI, thereby affecting
5 photosynthetic electron transfer and ROS/redox metabolism in the chloroplast.

6 ***O₂ sink roles of mitochondrial respiratory pathways***

7 The interaction between mitochondrial and chloroplastic ROS metabolism was previously
8 linked to the alternative respiratory pathway. This is supported by correlations between
9 chloroplastic phenotypes and AOX abundance and capacity (Fig. 6) and by the observation that
10 the AOX inhibitor SHAM alters photosynthetic electron flow and MV toxicity (Shapiguzov et
11 al., 2019; Pascual et al., 2021). However, the interaction could not be ascribed to a specific
12 AOX isoform. For example, the *AOX1a*-OE line does not display increased MV tolerance (Fig.
13 2; Shapiguzov et al., 2020), despite its high KCN-resistant AOX respiration (Fig. 5;
14 Shapiguzov et al., 2019). Single mutants *aox1a*, *aox1c*, and *aox1d*, as well as the double
15 mutant *aox1a aox1d* all show wild-type-like responses to MV (Supplementary Fig. 9B;
16 Shapiguzov et al., 2020). Furthermore, no differences in response to MV were observed
17 between *rcd1* and *rcd1 aox1a* (Shapiguzov et al., 2019; Shapiguzov et al., 2020). These results
18 suggest functional redundancy among AOX isoforms and point to a complex contribution of
19 various mitochondrial respiratory components to MV tolerance.

20 Indeed, the lines with induced MDS signaling exhibit a broad MDS transcriptional response,
21 with induced expression of several AOX and ND isoforms, the latter likely complementing
22 AOX activities (Sweetman et al., 2019) (Fig. 6C). Nitric oxide (NO) metabolism adds further
23 complexity: AOXs reduce electron leakage to nitrite under normoxia, suppressing NO
24 formation, while under hypoxia, over-reduced mitochondria can generate NO, which inhibits
25 COX. Increased NO emission under hypoxia was reported in AOX-overexpressing lines
26 (Jayawardhane et al., 2020; Vishwakarma et al., 2018), suggesting interplay between AOX and
27 COX via NO. However, in our assays, the *hot5* mutant and *GSNOR-GFP* line showed largely
28 wild-type-like responses, indicating that NO is not central to this interaction. The complexity
29 of the above regulatory network likely explains the controversial performance of the *AOX1a*-
30 OE transgenic line. While overexpression of *AOX1a* alone is sufficient to confer KCN-

1 resistant respiration, it is insufficient to reproduce the physiological changes observed in other
2 lines with mitochondrial defects.

3 Metabolic profiling of *rcd1* revealed increased respiratory flux (Shapiguzov et al., 2019) and
4 altered pools of primary metabolites, many of which are mitochondrial substrates (Sipari et al.,
5 2020). Hence, the molecular basis of mitochondrial O₂ sink capacity, and its impact on
6 chloroplasts, is likely context-dependent and shaped by the flexibility of different respiratory
7 branches (Sweetlove et al., 2010; Møller et al., 2021).

8 ***Possible implications and open questions***

9 We performed direct measurements of tissue O₂ status and chloroplastic phenotypes in a set of
10 Arabidopsis mutants and transgenic lines with diverse mitochondrial defects. Our study
11 proposes a mechanistic link between mitochondrial O₂ consumption and chloroplast
12 metabolism. While this interaction was revealed under artificial conditions using hypoxic
13 atmosphere and MV treatment, the constitutively altered redox states of chloroplast thiol
14 enzymes in *rcd1* suggest that the link is also relevant under natural conditions (Shapiguzov et
15 al., 2019; Shapiguzov et al., 2020). A recent study showed daily O₂ fluctuations in young
16 Arabidopsis leaves, with depletion at night due to respiration and accumulation during the day
17 driven by photosynthesis (Triozi et al., 2024). The effects of stressed mitochondrial
18 respiration on these dynamics remain to be explored.

19 The results of this study highlight the Mehler reaction as a key link coordinating respiration
20 and photosynthesis. The Mehler reaction controls chloroplast thiol redox states, thereby
21 regulating processes such as carbon fixation, sugar metabolism, and ATP production. It may be
22 required for activating photosynthetic electron transfer during the dark-to-light transition (Hani
23 et al., 2024) and it influences numerous signaling pathways dependent on chloroplast-derived
24 ROS (Shapiguzov et al., 2012; Wang et al., 2020). For instance, chloroplastic ROS are sensed
25 by the nuclear co-regulator RCD1, which interacts with transcription factors including
26 ANAC013/ANAC016/ANAC017 (mitochondrial signaling), ERFVIIIs (low-O₂ signaling), and
27 PIFs (light signaling) (Jaspers et al., 2009; Shapiguzov et al., 2019; Vainonen et al., 2023).
28 Furthermore, through its effect on photoassimilation, the Mehler reaction impacts sugar
29 signaling via SnRK1 and TOR pathways, which merge with hypoxic signaling (Kunkowska et
30 al., 2023). Future studies should explore how mitochondrial O₂ consumption shapes ROS

1 signaling across organelles and compartments, including the apoplast and nucleus (Shapiguzov
2 et al., 2012; Waszczak et al., 2018).

3 Our findings open opportunities for phenotyping plant respiration. In situ measurement of
4 mitochondrial respiration is challenging due to the lack of direct spectroscopic markers.
5 However, we show that mitochondrial activity can influence chlorophyll fluorescence under
6 certain conditions, providing an opportunity to infer respiratory traits via spectroscopic
7 approaches. This could form the basis for imaging tools to monitor plant respiration.

8 9 **Materials and Methods**

10 ***Plant material and growth conditions***

11 *Arabidopsis* (*Arabidopsis thaliana*) was used in all experiments. Plants were grown on either
12 1:1 mix of soil and vermiculite in 12 h photoperiod with 200-250 $\mu\text{mol m}^{-2} \text{s}^{-1}$ illumination
13 (low light growth conditions) or on MS plates (full-strength MS-medium, 0.6 % gel, 3 mM
14 MES hydrate) in 12 h photoperiod with 200 $\mu\text{mol m}^{-2} \text{s}^{-1}$ illumination. The following mutants
15 were used in the experiments: knockout mutants *rcd1-4* (AT1G32230), *rcd1-1 anac017*
16 (AT1G32230/AT1G34190; Ng et al., 2013; Shapiguzov et al., 2019), *shot1-2* (AT3G60400;
17 Kim et al., 2012), *hot5-2* (AT5G43940; Feechan et al., 2005; Lee et al., 2008), *rpoTnp-1*
18 (AT5G15700; Kühn et al., 2009), *lon1-2* (AT5G26860; Rigas et al., 2009), *drp3a drp3b*
19 (AT4G33650/AT2G14120; Fujimoto et al., 2009), *ndufal* (AT3G08610; Meyer et al., 2011),
20 *ndufs4* (AT5G67590; Meyer et al., 2009), *rug3-1* (AT5G60870; Kühn et al., 2011), *phb3*
21 (AT5G40770; Van Aken et al., 2007), *mic60-1* (AT4G39690; Michaud et al., 2016), *cat2*
22 (AT4G35090; Queval et al., 2007), *gox1*, *cat2 gox1* (AT4G35090/ AT3G14420; Kerchev et al.,
23 2016), and *rcd1 cat2* (Kaurilind et al., 2015). The double mutant *aox1a aox1d* was generated
24 by crossing the single mutant lines *aox1a* (AT3G22370; Umbach et al., 2005) and *aox1d*
25 (AT1G32350; GK-529D11). Transgenic lines included *atad3a1 atad3b1: ATAD3A1-GFP*
26 (AT3G03060; Kim et al., 2021), *GSNOR-GFP* (AT5G43940; Xu et al., 2013), *AOX1a*
27 overexpressor (AT3G22370; Umbach et al., 2005), *ANAC013* overexpressor (AT1G32870; De
28 Clercq et al., 2013), and RNAi mutant ATPQi (AT3G52300; Liu et al., 2021). All mutants and
29 transgenic lines are in Columbia-0 (Col-0) background.

1 *Chlorophyll fluorescence imaging*

2 Chlorophyll fluorescence imaging assays were performed with leaf discs that were prepared
3 similarly for all measurements. Leaf discs were placed on the surface of ultrapure water with
4 0.05% Tween-20, in the presence or absence of MV in the concentrations indicated in figure
5 panels. The discs were then incubated in darkness to facilitate uptake of MV for approximately
6 16 h before imaging. To minimize the effects of MV on photosynthesis, precautions were taken
7 not to expose plant material to any light prior to measurements.

8 MV-induced photoinhibition as well as quenching of Fm and light-adapted chlorophyll
9 fluorescence were assessed by chlorophyll fluorescence imaging using IMAGING-PAM M-
10 Series (Heinz Walz, Effeltrich, Germany). Photoinhibition protocols are described in
11 (Shapiguzov and Kangasjärvi, 2022). In brief, MV toxicity in leaf discs, prepared as described
12 above, was induced by repetitive 1-hour light periods (450 nm, $80 \mu\text{mol m}^{-2} \text{s}^{-1}$) each followed
13 by a 20 min dark period, then F_0 and F_m measurements. The resulting decay of maximal
14 quantum yield of Photosystem II (PSII) was calculated as $F_v/F_m = (F_m - F_0)/F_m$. Chlorophyll
15 fluorescence quenching routines are described in (Shapiguzov et al., 2020). In brief, an hypoxic
16 environment was introduced by flushing nitrogen gas over the prepared leaf discs; first for 20
17 min in darkness to acclimate the leaf discs, then continuously through the experiment. Imaging
18 of chlorophyll fluorescence was conducted under a saturating light pulse (F_m relaxation
19 measurement) followed by low-intensity actinic light (450 nm, $80 \mu\text{mol m}^{-2} \text{s}^{-1}$; light-adapted
20 fluorescence measurement). For flash-induced chlorophyll fluorescence imaging we used
21 PlantScreen SC Mobile System equipped with ultra-fast CMOS camera TOMI 3 with 20 μs
22 maximal frame rate of image acquisition (Photon Systems Instruments, Drásov, Czechia).
23 Imaging protocols are described in (Shapiguzov et al., 2020). In brief, samples were placed in
24 an airtight container that was continuously flooded with nitrogen gas, and the measurements
25 were performed through the transparent cover for hypoxic measurements. The time of exposure
26 to nitrogen gas was adjusted to reach a steady state chlorophyll fluorescence response. For each
27 assay we used leaf discs from at least 4-5 independent plants (for MV-treated samples) or 3
28 independent plants (for control samples), and the experiments were repeated twice
29 (photoinhibition and light-adapted fluorescence measurements) or three times (F_m relaxation
30 and flash-induced chlorophyll fluorescence imaging measurements), with similar results.

1 ***P700 oxidation measurements***

2 P700 analyses were done as described in (Shapiguzov et al., 2019). The detached leaves were
3 placed on the surface of ultrapure water with 0.05% Tween-20, in the presence or absence of 1
4 μM MV and incubated overnight in darkness. For the generation of an hypoxic atmosphere, the
5 leaves were next placed into transparent plastic bags with or without an AnaeroGen hypoxia
6 generator. Soda lime granules were added to the bags, as described in (Shapiguzov et al., 2020),
7 to avoid the possible effects of CO_2 generated by the reaction. The leaves were kept inside the
8 bags for 4 hours in darkness, after which light treatments and spectroscopic measurements were
9 performed through the plastic using DUAL-PAM-100 (Walz, Germany).

10 ***Shoot tissue O_2 consumption and production***

11 Shoot tissue O_2 dynamics were measured using the MicroRespiration system (Unisense,
12 Denmark). Plants were grown on MS plates for approximately 3 weeks. Their aerial parts were
13 cut off, weighed to obtain fresh mass, and inserted into 2 mL glass vials, which were filled with
14 analysis buffer (Smart and Barko solution, 0.6 mM MgSO_4 , 0.8 mM CaCl_2 , 1 mM KHCO_3
15 supplemented with 5 mM MES monohydrate). To restrict photorespiration as O_2 builds up
16 inside the vial, the analysis buffer was partially deoxygenated by mixing at 1:1 ratio O_2 -
17 saturated buffer and buffer that had been deoxygenated by bubbling it with nitrogen gas,
18 resulting in an initial O_2 concentration of approximately 150-200 $\mu\text{mol/L}$. The vials were
19 placed in a rack inside a constant temperature bath (37 °C) and O_2 concentrations were
20 monitored through a capillary in the glass lid with an optode (OPTO-MR, Unisense Denmark)
21 using LOGGER (Unisense, Denmark) at a rate of 1 Hz while the plants were treated to the
22 following regime: vials were kept in darkness until O_2 concentrations in all vials had been
23 reduced to $<10 \mu\text{mol/L}$, or until the O_2 concentration in at least one vial had remained at <1
24 $\mu\text{mol/L}$ for at most 20 min. After this, the vials were illuminated ($30 \mu\text{mol m}^{-2} \text{s}^{-1}$) until the O_2
25 concentrations within vials had plateaued, or at most 2 h. O_2 concentrations were recorded with
26 RATE (Unisense, Denmark), and O_2 consumption in darkness as well as re-accumulation in
27 light were normalized to fresh sample mass. At least 5 biological replicates were measured,
28 with the exception of *drp3a drp3b* and *rug3* (3 replicates each). For measurements in the
29 presence of SHAM, either dimethyl sulfoxide (DMSO; control) or 8 mM SHAM was added to
30 the analysis buffer at the beginning of the measurement. Contamination between samples was

1 avoided by rinsing the O₂ optode in fresh buffer after SHAM-containing samples were
2 measured.

3 *Leaf tissue O₂ dynamics*

4 O₂ status of intact leaves submerged in deoxygenated medium was measured using Clark-type
5 O₂ microsensors (Unisense, Denmark). Whole leaves were excised, kept submerged in 0.05%
6 Tween-20 solution overnight (12-16 h) in darkness, and placed over a firm foam with the main
7 vein facing upwards. A solid piece of plastic with a hole in the center was positioned over the
8 leaf, the sandwiched leaf was attached firmly to a metal mesh with rubber bands and placed
9 inside a container (200×100×100 mm, in total 2 L). An O₂ microsensor (OX-10, Unisense,
10 Denmark) was inserted 80-100 µm into the main vein of the leaf lamina, with 0 indicating the
11 tissue surface. Stagnant, deoxygenated buffer solution (0.1% agar) was added to the container
12 and O₂ concentration on the adaxial side of leaf central vein was recorded using LOGGER
13 (Unisense, Denmark) at a rate of 1 hz. The initial part of the measurement was conducted in
14 darkness, until the O₂ concentration declined and remained at a steady state below 5 µmol/L.
15 Then, a light was turned on (ca. 15 µmol m⁻² s⁻¹) and O₂ concentration was measured until it
16 reached a plateau. The O₂ concentration and temperature of the external medium were
17 monitored using an O₂ minioptode (OPTO-MR, Unisense, Denmark) and a temperature probe
18 (ZNTC, Unisense, Denmark). The positioning of the microsensor was aided by a motorized
19 micromanipulator controlled by LOGGER and visually aided with a dissection microscope
20 (WILD M3B, Leica, Switzerland).

21 *Protein abundance measurements*

22 Total AOX abundance was determined by immunoblotting. Untreated plants were grown on
23 either MS plates for 18 d and collected whole, or on soil for 21 d and their leaves were
24 collected. Plant tissue was ground in liquid nitrogen, and proteins were extracted by incubating
25 the samples for 20 min at 37 °C in lysis buffer (2% SDS, 20 mM Tris-HCl pH 7.8
26 supplemented with protease inhibitor cocktail P9599, Sigma-Aldrich). After centrifugation for
27 5 min at 15 000 g, the samples were suspended in Laemmli buffer. Protein amounts were
28 normalized to total protein (52.3 µg/well) or fresh plant mass (5 mg/well) for whole leaves and
29 seedlings, respectively. The extracts were separated on a 12% SDS-PAGE gel and transferred
30 to Bio-Rad Immun-blot PVDF membrane. AOX was detected with an αAOX1/2 antibody

1 (AS04 054, dil. 1:5000, Agrisera), PSI with an α PsaA antibody (AS06 172, dil. 1:5000,
2 Agrisera), together with an HRP-tagged secondary antibody (ECL anti-rabbit IgG
3 LNA934V/AH, GE Healthcare), and detected using a UVP Biospectrum 610 imaging system.
4 For total protein estimations, the membranes were stained with amido black. Band intensities
5 were calculated with the gel analyzer in ImageJ. Quantification was done using 4 independent
6 immunoblots.

7 ***Measurements of O₂ consumption rates in the presence of respiration inhibitors***

8 For measurements of plant O₂ consumption in the presence of respiration inhibitors, plants
9 were grown for 18 d on MS plates, aerial parts were cut off, weighed (approximately 20
10 mg/sample), and placed in an Oxygraph measurement chamber (Hansatech instruments) in air-
11 saturated liquid MS medium. Oxygen consumption in darkness was monitored with a Clark-
12 type O₂ electrode until it stabilized, for approximately 15 min. After this, changes in O₂
13 consumption were measured in the presence of respiration inhibitors by injecting potassium
14 cyanide (KCN, 4 mM) into the measurement chamber, waiting for the signal to stabilize, then
15 adding SHAM (2 mM) in the same manner. Respiratory parameters were processed with the
16 Oxygraph plus software, and relative O₂ consumption rates were determined by normalizing
17 the rates to plant mass. Six biological replicates were measured for each plant line.

18 ***Transcriptome analyses***

19 RNA sequence data were acquired from the publicly available NCBI GEO Datasets
20 (<https://www.ncbi.nlm.nih.gov/geo/>) for the following Arabidopsis mutant lines with
21 compromised mitochondria: *mtran1 mtran2* (Tran et al., 2023), *phb3* and *rpoTnp* (Van Aken et
22 al., 2016), two datasets with *rcd1* (Wirthmueller et al., 2018; Tao et al., 2023), *gsnor1* (Pan and
23 Cui, 2021) and *lon1* (Song et al., 2024). Only datasets with at least three biological replicates
24 were included in the analysis. For the paired-end sequences, each read end was processed
25 individually while retaining pairing information. The raw sequencing data underwent quality
26 control using FastQC (Andrews, 2010), followed by sequence trimming using Trimmomatic
27 (Bolger et al., 2014), to remove low-quality bases when necessary. Potential contamination
28 from ribosomal RNA was removed with sortmeRNA (Kopylova et al., 2012). The trimmed
29 reads were then aligned using STAR with the latest available Arabidopsis transcriptome

1 reference (AtRTD3) (Zhang et al., 2022). Differentially expressed genes were identified using
2 the DESeq2 package in Rstudio (Love et al., 2014).

3 ***Statistical analyses***

4 Statistical analyses of all results were conducted with SPSS (IBM, USA). Differences between
5 variances were estimated with ANOVA or Kruskal-Wallis, depending on the normality and
6 equality distributions of the samples. Correlation from average values was measured with
7 Bonferroni-corrected Pearson. Standard cut-off limit for statistically significant p-value (0.05)
8 was used for all experiments except correlation, where p-value 0.01 was used as well. The box
9 and whisker plots included in figures show the median (horizontal line), the first and third
10 quartiles (box), minimum and maximum (whiskers), and outliers, defined as 3rd quartile +
11 1.5*interquartile range and 1st quartile - 1.5*interquartile range (dots). Raw data and statistics
12 are presented in Supplementary Dataset S1.

14 **Accession Numbers**

15 TAIR gene identifiers corresponding to the mutants and overexpressor lines used in the study
16 are listed in Materials and Methods, *Plant material and growth conditions*. NCBI GEO
17 datasets used for transcriptome analyses are listed in Materials and Methods, *Transcriptome*
18 *analyses*.

20 **Author contributions**

21 M.P., B.B., O.B., L.L.P.O., M.K., M.B., L.N., E.V., O.P. and A.S. conceived and designed
22 experiments. M.P., B.B., L.L.P.O., M.K., M.B., L.N. and A.S. carried out experiments. All
23 authors analyzed the results. A.S. and M.P. wrote the article. All authors read and contributed to
24 the final article.

26 **Funding**

27 This work was supported by the Centre of Excellence in Tree Biology, Research Council of
28 Finland (decision 346140; A.S.). Development of *ATAD3-GFP*, *ATPd* RNAi line, *hot5-2*, and

1 *GSNOR-GPF* lines were supported by United States National Science Foundation grants IOS
2 1354960 and MCB 1517046 to E.V.

4 **Acknowledgments**

5 The authors dedicate this study to the memory of Prof. Jaakko Kangasjärvi. We thank Prof.
6 Romy Schmidt-Schippers for the advice on the studies of hypoxia and for her critical
7 comments on the manuscript. We thank Dr. Cezary Waszczak for sharing the seeds of
8 photorespiratory mutants and Dr. Julia Vainonen for the help in the preparation of this
9 manuscript.

11 **Figure legends**

12 **Figure 1. Diagram of mutants and transgenic lines used in the study.** We utilized a set of
13 mutants and transgenic lines with a wide variety of mitochondrial perturbations to examine the
14 interactions between mitochondrial respiration and the chloroplastic Mehler reaction (purple
15 arrow). The mutants and transgenic lines are written in italics next to the affected functions,
16 pathways or complexes. References for all lines are provided in Materials and Methods.

18 **Figure 2. MV-induced responses in plant lines with perturbed mitochondrial functions.**

19 (A, B) MV-induced photoinhibition. Repeated exposure of MV-treated leaf discs to light led to
20 a gradual decline of maximal PSII quantum yield (F_v/F_m) in susceptible genotypes such as
21 Col-0, while other lines retained PSII function. The kinetics of F_v/F_m in selected MV-tolerant
22 lines compared to wild type during long-term illumination are shown in (A) as averages (\pm SD)
23 measured from at least 4 individual plants. F_v/F_m values for all tested lines at the 15 h time
24 point are shown in (B), with box plots indicating the median (horizontal line), 1st and 3rd
25 quartiles (box), and minimum and maximum (whiskers) arranged in order of increasing mean.
26 Statistically significant groups (Kruskal-Wallis test, $p < 0.05$) are indicated with letters, bolded
27 for plant lines that have higher F_v/F_m than the wild type. (C–F) MV-induced quenching of
28 chlorophyll fluorescence under hypoxia. Several plant lines displayed resistance to MV-
29 induced chlorophyll fluorescence decay under hypoxic atmosphere, in contrast to MV-sensitive

1 lines such as Col-0. This was observed both in dark relaxation of Fm (C, D) and in light-
2 adapted fluorescence under actinic light (E, F). Values shown in (C, E) are averages (\pm SD), the
3 box plots (D, F) indicate the median (horizontal line), 1st and 3rd quartiles (box), minimum and
4 maximum (whiskers) measured from at least 5 individual plants. Kinetics of chlorophyll
5 fluorescence in selected lines are shown in (C, E); image (C) is a magnified view of the first 50
6 seconds of (E). Fluorescence responses were quantified by calculating the integrated area under
7 the curve for dark relaxation of Fm (D) and light-adapted fluorescence (F), with genotypes
8 arranged in order of increasing mean. Statistically significant groups are indicated with letters;
9 bolded letters indicate lines with higher remaining chlorophyll fluorescence than the wild type
10 (Kruskal-Wallis test, $p < 0.05$). Both sets of experiments were repeated twice with similar
11 results. MV, methyl viologen.

12
13 **Figure 3. Photosystem I (PSI) oxidation in the presence of MV under hypoxic conditions**
14 **in plant lines with perturbed mitochondrial functions.** P700 reoxidation kinetics after a

15 saturating flash of red (Photosystem II-specific) light (red arrow) over the far-red (PSI-
16 specific) background in leaves pre-treated with MV or untreated are shown in (A). P700
17 dynamics were quantified by measuring the time required to reach 50% of the initial P700
18 oxidation level after the red flash (B). Statistically significant difference between hypoxic
19 results (Mann-Whitney U test, $p < 0.05$) is indicated with an asterisk. Values are averages (\pm
20 SD) from at least 4 individual plants. No statistically significant differences were detected in
21 PSI abundance in total leaf extracts assessed by immunoblotting with an α PsaA antibody.
22 Values are averages (\pm SD) from at least 4 individual plants. The PsaA signal was normalized
23 to *rcd1* (C). OJIP kinetics were determined to examine the effects of MV directly on the
24 electron-acceptor side of PSI. Kinetics in selected lines under hypoxic conditions in leaf discs
25 treated with 2 μ M MV are shown in (D). Quantification of ϕ RE1o was used as an indicator of
26 the I-P rise, corresponding to PSI activity (E). Values are averages (\pm SD) from at least 4
27 individual plants with genotypes arranged in the order of increasing mean under MV.
28 Statistically significant groups are indicated with letters, bolded for lines that have higher
29 ϕ RE1o value in the presence of MV than wild type (Kruskal-Wallis test, $p < 0.05$). The
30 experiment was performed three times with similar results. MV, methyl viologen.

31

1 **Figure 4. O₂ consumption and accumulation dynamics in plant lines with perturbed**
2 **mitochondrial functions.** O₂ dynamics in selected plant lines were examined by measuring O₂
3 fluctuations in cuvettes where aerial parts of plate-grown plants were immersed in analysis
4 buffer. An example of this assay performed with Col-0 and *rcd1* is shown in (A), with relative
5 O₂ consumption rate first recorded in darkness. After O₂ concentrations approached zero, the
6 light was turned on (vertical line at approx. 30 min) and O₂ re-accumulation caused by
7 photosynthetic O₂ evolution was recorded. Consumption (B) and re-accumulation (C) rates of
8 O₂ were obtained from the kinetics as shown in (A). The box plots indicate the median
9 (horizontal line), 1st and 3rd quartiles (box), minimum and maximum (whiskers) measured in at
10 least 3 replicates, with each replicate consisting of several individual seedling aerial parts. The
11 genotypes are arranged in order of increasing mean in (B), and in (C) they are in the same
12 order as in (B). Statistically significant groups are indicated with letters, which are bolded for
13 lines that have higher O₂ consumption or lower O₂ re-accumulation rates than wild type
14 (Kruskal-Wallis test, $p < 0.05$).

15
16 **Figure 5. AOX abundance and capacity in plant lines with perturbed mitochondrial**
17 **functions.** AOX abundance was measured by immunoblotting total protein extracts from
18 seedlings (A), and AOX capacity was determined as the fraction of O₂ consumption that was
19 not inhibited by KCN (B). The box plots indicate the median (horizontal line), 1st and 3rd
20 quartiles (box), minimum and maximum (whiskers), and the genotypes are arranged in order of
21 increasing mean. Statistically significant groups are indicated with letters, bolded for lines that
22 are different from the wild type (Kruskal-Wallis test, $p < 0.05$). Quantification in (A) was from
23 4 independent immunoblots, and in (B) from 6 independent biological replicates. Correlation
24 between AOX abundance and capacity is displayed in (C).

25
26 **Figure 6. Correlation of chloroplastic and mitochondrial phenotypes and expression of**
27 **alternative respiratory enzymes in plant lines with perturbed mitochondrial functions.**
28 Parameters associated with chloroplastic and mitochondrial phenotypes were analyzed using
29 Pearson correlation, excluding the atypically behaving *AOX1a*-OE line (A). Correlation values
30 are bolded and marked with one or two asterisks to indicate significance at $p < 0.05$ and < 0.01 ,

1 respectively, and the color of the pane is used to indicate the strength and direction of
2 correlation. Plant lines included in the correlation analyses in panel (A) are listed in (B).
3 Details are available in Supplementary Dataset S1. (C) Publicly available transcriptome
4 datasets were re-analyzed to identify genes with significantly altered expression. Data are
5 presented as the fold change in the mutant relative to the wild type. Displayed are *AOX*, *ND*,
6 and marker genes for MDS (*UPOX* and *HRG2*), and hypoxia (*ERF71*, *HRU1*, *PDC1*). MV,
7 methyl viologen. CF, chlorophyll fluorescence.

9 References

- 10 Abbas, M., Sharma, G., Dambire, C., Marquez, J., Alonso-Blanco, C., Proaño, K., & Holdsworth, M. J. (2022).
11 An oxygen-sensing mechanism for angiosperm adaptation to altitude. *Nature*, 606(7914), 565–569.
12 <https://doi.org/10.1038/s41586-022-04740-y>
- 13 Andrews, S. (2010). FastQC: A Quality Control Tool for High Throughput Sequence Data [Online]. Available
14 online at: <http://www.bioinformatics.babraham.ac.uk/projects/fastqc/>.
- 15 Bailleul, B., Berne, N., Murik, O., Petroustos, D., Prihoda, J., Tanaka, A., Villanova, V., Bligny, R., Flori, S.,
16 Falconet, D., Krieger-Liszkay, A., Santabarbara, S., Rappaport, F., Joliot, P., Tirichine, L., Falkowski, P. G.,
17 Cardol, P., Bowler, C., & Finazzi, G. (2015). Energetic coupling between plastids and mitochondria drives CO₂
18 assimilation in diatoms. *Nature*, 524(7565), 366–369. <https://doi.org/10.1038/nature14599>
- 19 Bailey-Serres, J., Geigenberger, P., Perata, P., Sasidharan, R., & Schwarzländer, M. (2024). Hypoxia as challenge
20 and opportunity: From cells to crops, to synthetic biology. *Plant physiology*, 197(1), kiae640.
21 <https://doi.org/10.1093/plphys/kiac640>
- 22 Bauwe, H., Hagemann, M., & Fiering, A. R. (2010). Photorespiration: players, partners and origin. *Trends in plant*
23 *science*, 15(6), 330–336. <https://doi.org/10.1016/j.tplants.2010.03.006>
- 24 Bolger, A. M., Lohse, M., & Usadel, B. (2014). Trimmomatic: a flexible trimmer for Illumina sequence data.
25 *Bioinformatics (Oxford, England)*, 30(15), 2114–2120. <https://doi.org/10.1093/bioinformatics/btu170>
- 26 Brosché, M., Blomster, T., Salojärvi, J., Cui, F., Sipari, N., Leppälä, J., Lamminmäki, A., Tomai, G.,
27 Narayanasamy, S., Reddy, R. A., Keinänen, M., Overmyer, K., & Kangasjärvi, J. (2014). Transcriptomics and
28 functional genomics of ROS-induced cell death regulation by RADICAL-INDUCED CELL DEATH1. *PLoS*
29 *genetics*, 10(2), e1004112. <https://doi.org/10.1371/journal.pgen.1004112>
- 30 Dahal, K., & Vanlerberghe, G. C. (2017). Alternative oxidase respiration maintains both mitochondrial and
31 chloroplast function during drought. *The New phytologist*, 213(2), 560–571. <https://doi.org/10.1111/nph.14169>
- 32 De Clercq, I., Vermeirssen, V., Van Aken, O., Vandepoele, K., Murcha, M. W., Law, S. R., Inzé, A., Ng, S.,
33 Ivanova, A., Rombaut, D., van de Cotte, B., Jaspers, P., Van de Peer, Y., Kangasjärvi, J., Whelan, J., & Van
34 Breusegem, F. (2013). The membrane-bound NAC transcription factor ANAC013 functions in mitochondrial
35 retrograde regulation of the oxidative stress response in *Arabidopsis*. *The Plant cell*, 25(9), 3472–3490.
36 <https://doi.org/10.1105/tpc.113.117168>

- 1 Farrington, J. A., Ebert, M., Land, E. J., & Fletcher, K. (1973). Bipyridylum quaternary salts and related
2 compounds. V. Pulse radiolysis studies of the reaction of paraquat radical with oxygen. Implications for the mode
3 of action of bipyridyl herbicides. *Biochimica et Biophysica Acta (BBA)-Bioenergetics*, 314(3), 372-381.
- 4 Eysholdt-Derzsó, E., Renziehausen, T., Frings, S., Frohn, S., von Bongartz, K., Igisch, C. P., Mann, J., Häger, L.,
5 Macholl, J., Leisse, D., Hoffmann, N., Winkels, K., Wanner, P., De Backer, J., Luo, X., Sauter, M., De Clercq, I.,
6 van Dongen, J. T., Schippers, J. H. M., & Schmidt-Schippers, R. R. (2023). Endoplasmic reticulum-bound
7 ANAC013 factor is cleaved by RHOMBOID-LIKE 2 during the initial response to hypoxia in *Arabidopsis*
8 *thaliana*. *Proceedings of the National Academy of Sciences of the United States of America*, 120(11),
9 e2221308120. <https://doi.org/10.1073/pnas.2221308120>
- 10 Feechan, A., Kwon, E., Yun, B. W., Wang, Y., Pallas, J. A., & Loake, G. J. (2005). A central role for S-
11 nitrosothiols in plant disease resistance. *Proceedings of the National Academy of Sciences of the United States of*
12 *America*, 102(22), 8054–8059. <https://doi.org/10.1073/pnas.0501456102>
- 13 Fujimoto, M., Arimura, S., Mano, S., Kondo, M., Saito, C., Ueda, T., Nakazono, M., Nakano, A., Nishimura, M.,
14 & Tsutsumi, N. (2009). *Arabidopsis* dynamin-related proteins DRP3A and DRP3B are functionally redundant in
15 mitochondrial fission, but have distinct roles in peroxisomal fission. *The Plant journal : for cell and molecular*
16 *biology*, 58(3), 388–400. <https://doi.org/10.1111/j.1365-313X.2009.03786.x>
- 17 Gupta, K. J., Zabalza, A., & van Dongen, J. T. (2009). Regulation of respiration when the oxygen availability
18 changes. *Physiologia plantarum*, 137(4), 383–391. <https://doi.org/10.1111/j.1399-3054.2009.01253.x>
- 19 Gupta, K. J., Kumari, A., Florez-Sarasa, I., Fernie, A. R., & Igamberdiev, A. U. (2018). Interaction of nitric oxide
20 with the components of the plant mitochondrial electron transport chain. *Journal of experimental botany*, 69(14),
21 3413–3424. <https://doi.org/10.1093/jxb/ery119>
- 22 Hani, U., Naranjo, B., Shimakawa, G., Espinasse, C., Vanacker, H., Sétif, P., Rintamäki, E., Issakidis-Bourguet,
23 E., & Krieger-Liszka, A. (2024). A complex and dynamic redox network regulates oxygen reduction at
24 photosystem I in *Arabidopsis*. *Plant physiology*, 197(1), kiae501. <https://doi.org/10.1093/plphys/kiae501>
- 25 Iida, H., Abreu, I., López Ortiz, J., Peralta Ogorek, L. L., Shukla, V., Mäkelä, M., Lyu, M., Shapiguzov, A.,
26 Licausi, F., & Mähönen, A. P. (2025). Plants monitor the integrity of their barrier by sensing gas diffusion. *Nature*,
27 10.1038/s41586-025-09223-4. Advance online publication. <https://doi.org/10.1038/s41586-025-09223-4>
- 28 Jayawardhane, J., Cochrane, D. W., Vyas, P., Bykova, N. V., Vanlerberghe, G. C., & Igamberdiev, A. U. (2020).
29 Roles for Plant Mitochondrial Alternative Oxidase Under Normoxia, Hypoxia, and Reoxygenation Conditions.
30 *Frontiers in plant science*, 11, 566. <https://doi.org/10.3389/fpls.2020.00566>
- 31 Jaspers, P., Blomster, T., Brosché, M., Salojärvi, J., Ahlfors, R., Vainonen, J. P., Reddy, R. A., Immink, R.,
32 Angenent, G., Turck, F., Overmyer, K., & Kangasjärvi, J. (2009). Unequally redundant RCD1 and SRO1 mediate
33 stress and developmental responses and interact with transcription factors. *The Plant journal : for cell and*
34 *molecular biology*, 60(2), 268–279. <https://doi.org/10.1111/j.1365-313X.2009.03951.x>
- 35 Jethva, J., Schmidt, R. R., Sauter, M., & Selinski, J. (2022). Try or Die: Dynamics of Plant Respiration and How
36 to Survive Low Oxygen Conditions. *Plants (Basel, Switzerland)*, 11(2), 205.
37 <https://doi.org/10.3390/plants11020205>
- 38 Kaurilind, E., Xu, E., & Brosché, M. (2015). A genetic framework for H₂O₂ induced cell death in *Arabidopsis*
39 *thaliana*. *BMC genomics*, 16, 837. <https://doi.org/10.1186/s12864-015-1964-8>
- 40 Kelliher, T., & Walbot, V. (2012). Hypoxia triggers meiotic fate acquisition in maize. *Science (New York, N.Y.)*,
41 337(6092), 345–348. <https://doi.org/10.1126/science.1220080>

- 1 Kerchev, P., Waszczak, C., Lewandowska, A., Willems, P., Shapiguzov, A., Li, Z., Alseekh, S., Mühlenbock, P.,
2 Hoeberichts, F. A., Huang, J., Van Der Kelen, K., Kangasjärvi, J., Fernie, A. R., De Smet, R., Van de Peer, Y.,
3 Messens, J., & Van Breusegem, F. (2016). Lack of GLYCOLATE OXIDASE1, but Not GLYCOLATE
4 OXIDASE2, Attenuates the Photorespiratory Phenotype of CATALASE2-Deficient Arabidopsis. *Plant physiology*,
5 171(3), 1704–1719. <https://doi.org/10.1104/pp.16.00359>
- 6 Khan, K., Tran, H. C., Mansuroglu, B., Önsell, P., Buratti, S., Schwarzländer, M., Costa, A., Rasmusson, A. G., &
7 Van Aken, O. (2024). Mitochondria-derived reactive oxygen species are the likely primary trigger of
8 mitochondrial retrograde signaling in Arabidopsis. *Current biology : CB*, 34(2), 327–342.e4.
9 <https://doi.org/10.1016/j.cub.2023.12.005>
- 10 Kim, M., Lee, U., Small, I., des Francs-Small, C. C., & Vierling, E. (2012). Mutations in an Arabidopsis
11 mitochondrial transcription termination factor-related protein enhance thermotolerance in the absence of the major
12 molecular chaperone HSP101. *The Plant cell*, 24(8), 3349–3365. <https://doi.org/10.1105/tpc.112.101006>
- 13 Kim, M., Schulz, V., Brings, L., Schoeller, T., Kühn, K., & Vierling, E. (2021). mTERF18 and ATAD3 are
14 required for mitochondrial nucleoid structure and their disruption confers heat tolerance in Arabidopsis thaliana.
15 *The New phytologist*, 232(5), 2026–2042. <https://doi.org/10.1111/nph.17717>
- 16 Kopylova, E., Noé, L., & Touzet, H. (2012). SortMeRNA: fast and accurate filtering of ribosomal RNAs in
17 metatranscriptomic data. *Bioinformatics (Oxford, England)*, 28(24), 3211–3217.
18 <https://doi.org/10.1093/bioinformatics/bts611>
- 19 Kunkowska, A. B., Fontana, F., Betti, F., Soeur, R., Beckers, G. J. M., Meyer, C., De Jaeger, G., Weits, D. A.,
20 Loreti, E., & Perata, P. (2023). Target of rapamycin signaling couples energy to oxygen sensing to modulate
21 hypoxic gene expression in Arabidopsis. *Proceedings of the National Academy of Sciences of the United States of*
22 *America*, 120(3), e2212474120. <https://doi.org/10.1073/pnas.2212474120>
- 23 Kühn, K., Richter, U., Meyer, E. H., Delannoy, E., de Longevialle, A. F., O'Toole, N., Börner, T., Millar, A. H.,
24 Small, I. D., & Whelan, J. (2009). Phage-type RNA polymerase RPOTmp performs gene-specific transcription in
25 mitochondria of Arabidopsis thaliana. *The Plant cell*, 21(9), 2762–2779. <https://doi.org/10.1105/tpc.109.068536>
- 26 Kühn, K., Carrie, C., Giraud, E., Wang, Y., Meyer, E. H., Narsai, R., des Francs-Small, C. C., Zhang, B., Murcha,
27 M. W., & Whelan, J. (2011). The RCC1 family protein RUG3 is required for splicing of nad2 and complex I
28 biogenesis in mitochondria of Arabidopsis thaliana. *The Plant journal : for cell and molecular biology*, 67(6),
29 1067–1080. <https://doi.org/10.1111/j.1365-313X.2011.04658.x>
- 30 Lee, U., Wie, C., Fernandez, B. O., Feelisch, M., & Vierling, E. (2008). Modulation of nitrosative stress by S-
31 nitrosoglutathione reductase is critical for thermotolerance and plant growth in Arabidopsis. *The Plant cell*, 20(3),
32 786–802. <https://doi.org/10.1105/tpc.107.052647>
- 33 Liu, T., Arsenault, J., Vierling, E., & Kim, M. (2021). Mitochondrial ATP synthase subunit d, a component of the
34 peripheral stalk, is essential for growth and heat stress tolerance in Arabidopsis thaliana. *The Plant journal : for*
35 *cell and molecular biology*, 107(3), 713–726. <https://doi.org/10.1111/tpj.15317>
- 36 Love, M. I., Huber, W., & Anders, S. (2014). Moderated estimation of fold change and dispersion for RNA-seq
37 data with DESeq2. *Genome biology*, 15(12), 550. <https://doi.org/10.1186/s13059-014-0550-8>
- 38 Meyer, E. H., Tomaz, T., Carroll, A. J., Estavillo, G., Delannoy, E., Tanz, S. K., Small, I. D., Pogson, B. J., &
39 Millar, A. H. (2009). Remodeled respiration in ndufs4 with low phosphorylation efficiency suppresses
40 Arabidopsis germination and growth and alters control of metabolism at night. *Plant physiology*, 151(2), 603–619.
41 <https://doi.org/10.1104/pp.109.141770>

- 1 Meyer, E. H., Solheim, C., Tanz, S. K., Bonnard, G., & Millar, A. H. (2011). Insights into the composition and
2 assembly of the membrane arm of plant complex I through analysis of subcomplexes in *Arabidopsis* mutant lines.
3 *The Journal of biological chemistry*, 286(29), 26081–26092. <https://doi.org/10.1074/jbc.M110.209601>
- 4 Michaud, M., Gros, V., Tardif, M., Brugière, S., Ferro, M., Prinz, W. A., Toulmay, A., Mathur, J., Wozny, M.,
5 Falconet, D., Maréchal, E., Block, M. A., & Jouhet, J. (2016). AtMic60 Is Involved in Plant Mitochondria Lipid
6 Trafficking and Is Part of a Large Complex. *Current biology : CB*, 26(5), 627–639.
7 <https://doi.org/10.1016/j.cub.2016.01.011>
- 8 Miyake C. (2010). Alternative electron flows (water-water cycle and cyclic electron flow around PSI) in
9 photosynthesis: molecular mechanisms and physiological functions. *Plant & cell physiology*, 51(12), 1951–1963.
10 <https://doi.org/10.1093/pcp/pcq173>
- 11 Murik, O., Tirichine, L., Prihoda, J., Thomas, Y., Araújo, W. L., Allen, A. E., Fernie, A. R., & Bowler, C. (2019).
12 Downregulation of mitochondrial alternative oxidase affects chloroplast function, redox status and stress response
13 in a marine diatom. *The New phytologist*, 221(3), 1303–1316. <https://doi.org/10.1111/nph.15479>
- 14 Møller, I. M., Rasmusson, A. G., & Van Aken, O. (2021). Plant mitochondria - past, present and future. *The Plant*
15 *journal : for cell and molecular biology*, 108(4), 912–959. <https://doi.org/10.1111/tpj.15495>
- 16 Nawrocki, W. J., Tourasse, N. J., Taly, A., Rappaport, F., & Wollman, F. A. (2015). The plastid terminal oxidase:
17 its elusive function points to multiple contributions to plastid physiology. *Annual review of plant biology*, 66, 49–
18 74. <https://doi.org/10.1146/annurev-arplant-043014-114744>
- 19 Ng, S., Ivanova, A., Duncan, O., Law, S. R., Van Aken, O., De Clercq, I., Wang, Y., Carrie, C., Xu, L., Kmiec, B.,
20 Walker, H., Van Breusegem, F., Whelan, J., & Giraud, E. (2013). A membrane-bound NAC transcription factor,
21 ANAC017, mediates mitochondrial retrograde signaling in *Arabidopsis*. *The Plant cell*, 25(9), 3450–3471.
22 <https://doi.org/10.1105/tpc.113.113985>
- 23 Nikkanen, L., Wey, L. T., Woodford, R., Mustila, H., Kosmützy, D., Ermakova, M., ... & Allahverdiyeva, Y.
24 (2024). PGR5 is needed for redox-dependent regulation of ATP synthase both in chloroplasts and in
25 cyanobacteria. *bioRxiv*, 2024-11. <https://doi.org/10.1101/2024.11.03.621747>
- 26 Nishiyama, Y., Allakhverdiev, S. I., & Murata, N. (2011). Protein synthesis is the primary target of reactive
27 oxygen species in the photoinhibition of photosystem II. *Physiologia Plantarum*, 142(1), 35–46.
28 <https://doi.org/10.1111/j.1399-3054.2011.01457.x>
- 29 Oh, G. G. K., O'Leary, B. M., Signorelli, S., & Millar, A. H. (2022). Alternative oxidase (AOX) 1a and 1d limit
30 proline-induced oxidative stress and aid salinity recovery in *Arabidopsis*. *Plant physiology*, 188(3), 1521–1536.
31 <https://doi.org/10.1093/plphys/kiab578>
- 32 Ojeda, V., Pérez-Ruiz, J. M., & Cejudo, F. J. (2018). 2-Cys Peroxiredoxins Participate in the Oxidation of
33 Chloroplast Enzymes in the Dark. *Molecular plant*, 11(11), 1377–1388.
34 <https://doi.org/10.1016/j.molp.2018.09.005>
- 35 Pan, Q., & Cui, B. (2021). RNA-sequence of *Arabidopsis thaliana* lines *gsnor1* and Col-0 post infection of
36 *Phytophthora parasitica* against controls. *BioStudies*, E-MTAB-8845.
37 <https://www.ebi.ac.uk/biostudies/arrayexpress/studies/E-MTAB-8845>
- 38 Pascual, J., Rahikainen, M., Angeleri, M., Alegre, S., Gossens, R., Shapiguzov, A., Heinonen, A., Trotta, A.,
39 Durian, G., Winter, Z., Sinkkonen, J., Kangasjärvi, J., Whelan, J., & Kangasjärvi, S. (2021). ACONITASE 3 is
40 part of the ANAC017 transcription factor-dependent mitochondrial dysfunction response. *Plant physiology*,
41 186(4), 1859–1877. <https://doi.org/10.1093/plphys/kiab225>

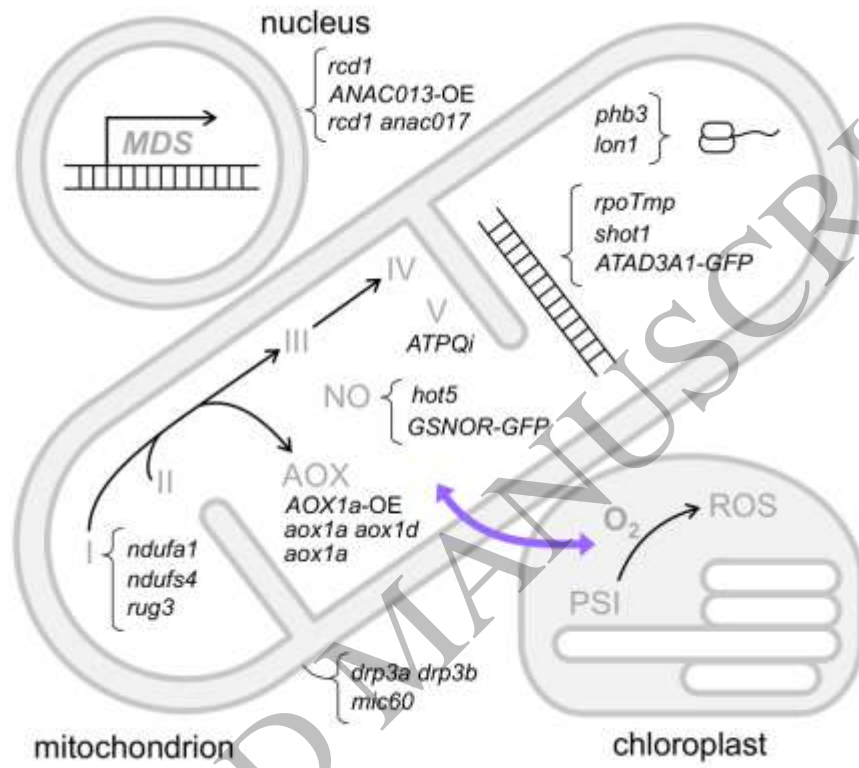
- 1 Queval, G., Issakidis-Bourguet, E., Hoeberichts, F. A., Vandorpe, M., Gakière, B., Vanacker, H., Miginiac-
2 Maslow, M., Van Breusegem, F., & Noctor, G. (2007). Conditional oxidative stress responses in the Arabidopsis
3 photorespiratory mutant *cat2* demonstrate that redox state is a key modulator of daylength-dependent gene
4 expression, and define photoperiod as a crucial factor in the regulation of H₂O₂-induced cell death. *The Plant*
5 *journal: for cell and molecular biology*, 52(4), 640–657. <https://doi.org/10.1111/j.1365-313X.2007.03263.x>
- 6 Rasmusson, A. G., Fernie, A. R., & van Dongen, J. T. (2009). Alternative oxidase: a defence against metabolic
7 fluctuations? *Physiologia plantarum*, 137(4), 371–382. <https://doi.org/10.1111/j.1399-3054.2009.01252.x>
- 8 Rigas, S., Daras, G., Laxa, M., Marathias, N., Fasseas, C., Sweetlove, L. J., & Hatzopoulos, P. (2009). Role of
9 Lon1 protease in post-germinative growth and maintenance of mitochondrial function in Arabidopsis thaliana. *The*
10 *New phytologist*, 181(3), 588–600. <https://doi.org/10.1111/j.1469-8137.2008.02701.x>
- 11 Renziehausen, T., Chaudhury, R., Hartman, S., Mustroph, A., & Schmidt-Schippers, R. R. (2024). A mechanistic
12 integration of hypoxia signaling with energy, redox, and hormonal cues. *Plant physiology*, 197(1), kiae596.
13 <https://doi.org/10.1093/plphys/kiad596>
- 14 Schreiber, U., & Klughammer, C. (2021). Evidence for variable chlorophyll fluorescence of photosystem I in
15 vivo. *Photosynthesis research*, 149(1-2), 213–231. <https://doi.org/10.1007/s11120-020-00814-y>
- 16 Schreiber U. (2023). Light-induced changes of far-red excited chlorophyll fluorescence: further evidence for
17 variable fluorescence of photosystem I in vivo. *Photosynthesis research*, 155(3), 247–270.
18 <https://doi.org/10.1007/s11120-022-00994-9>
- 19 Shameer, S., Ratcliffe, R. G., & Sweetlove, L. J. (2019). Leaf Energy Balance Requires Mitochondrial Respiration
20 and Export of Chloroplast NADPH in the Light. *Plant physiology*, 180(4), 1947–1961.
21 <https://doi.org/10.1104/pp.19.00624>
- 22 Shapiguzov, A., Vainonen, J. P., Wrzaczek, M., & Kangasjärvi, J. (2012). ROS-talk - how the apoplast, the
23 chloroplast, and the nucleus get the message through. *Frontiers in plant science*, 3, 292.
24 <https://doi.org/10.3389/fpls.2012.00292>
- 25 Shapiguzov, A., Vainonen, J. P., Hunter, K., Tossavainen, H., Tiwari, A., Järvi, S., Hellman, M., Aarabi, F.,
26 Alseekh, S., Wybouw, B., Van Der Kelen, K., Nikkanen, L., Krasensky-Wrzaczek, J., Sipari, N., Keinänen, M.,
27 Tyystjärvi, E., Rintamäki, E., De Rybel, B., Salojärvi, J., Van Breusegem, F., ... Kangasjärvi, J. (2019).
28 Arabidopsis RCD1 coordinates chloroplast and mitochondrial functions through interaction with ANAC
29 transcription factors. *eLife*, 8, e43284. <https://doi.org/10.7554/eLife.43284>
- 30 Shapiguzov, A., Nikkanen, L., Fitzpatrick, D., Vainonen, J. P., Gossens, R., Alseekh, S., Aarabi, F., Tiwari, A.,
31 Blokhina, O., Panzarová, K., Benedikty, Z., Tyystjärvi, E., Fernie, A. R., Trtílek, M., Aro, E. M., Rintamäki, E., &
32 Kangasjärvi, J. (2020). Dissecting the interaction of photosynthetic electron transfer with mitochondrial signalling
33 and hypoxic response in the Arabidopsis *red1* mutant. *Philosophical transactions of the Royal Society of London.*
34 *Series B, Biological sciences*, 375(1801), 20190413. <https://doi.org/10.1098/rstb.2019.0413>
- 35 Shapiguzov, A., & Kangasjärvi, J. (2022). Studying Plant Stress Reactions In Vivo by PAM Chlorophyll
36 Fluorescence Imaging. *Methods in molecular biology (Clifton, N.J.)*, 2526, 43–61. https://doi.org/10.1007/978-1-0716-2469-2_4
- 38 Sipari, N., Lihavainen, J., Shapiguzov, A., Kangasjärvi, J., & Keinänen, M. (2020). Primary Metabolite Responses
39 to Oxidative Stress in Early-Senescing and Paraquat Resistant Arabidopsis thaliana *red1* (Radical-Induced Cell
40 Death1). *Frontiers in plant science*, 11, 194. <https://doi.org/10.3389/fpls.2020.00194>
- 41 Song, C., Li, Y., Yang, M., Li, T., Hou, Y., Liu, Y., Xu, C., Liu, J., Millar, A. H., Wang, N., & Li, L. (2024). Protein
42 aggregation in plant mitochondria lacking Lon1 inhibits translation and induces unfolded protein responses. *Plant,*
43 *cell & environment*, 47(11), 4383–4397. <https://doi.org/10.1111/pce.15035>

- 1 Stirbet, A., & Govindjee (2011). On the relation between the Kautsky effect (chlorophyll a fluorescence induction)
2 and Photosystem II: basics and applications of the OJIP fluorescence transient. *Journal of photochemistry and*
3 *photobiology. B, Biology*, 104(1-2), 236–257. <https://doi.org/10.1016/j.jphotobiol.2010.12.010>
- 4 Stirbet, A., & Govindjee (2012). Chlorophyll a fluorescence induction: a personal perspective of the thermal
5 phase, the J-I-P rise. *Photosynthesis research*, 113(1-3), 15–61. <https://doi.org/10.1007/s11120-012-9754-5>
- 6 Strasser, R.J., Tsimilli-Michael, M., Srivastava, A. (2004). Analysis of the Chlorophyll a Fluorescence Transient.
7 In: Papageorgiou, G.C., Govindjee (eds) *Chlorophyll a Fluorescence. Advances in Photosynthesis and*
8 *Respiration*, vol 19. Springer, Dordrecht. https://doi.org/10.1007/978-1-4020-3218-9_12
- 9 Sweetlove, L. J., Beard, K. F., Nunes-Nesi, A., Fernie, A. R., & Ratcliffe, R. G. (2010). Not just a circle: flux
10 modes in the plant TCA cycle. *Trends in plant science*, 15(8), 462–470.
11 <https://doi.org/10.1016/j.tplants.2010.05.006>
- 12 Sweetman, C., Waterman, C. D., Rainbird, B. M., Smith, P. M. C., Jenkins, C. D., Day, D. A., & Soole, K. L.
13 (2019). AtNDB2 Is the Main External NADH Dehydrogenase in Mitochondria and Is Important for Tolerance to
14 Environmental Stress. *Plant physiology*, 181(2), 774–788. <https://doi.org/10.1104/pp.19.00877>
- 15 Tao, J., Wu, F., Wen, H., Liu, X., Luo, W., Gao, L., Jiang, Z., Mo, B., Chen, X., Kong, W., & Yu, Y. (2023). RCD1
16 Promotes Salt Stress Tolerance in Arabidopsis by Repressing ANAC017 Activity. *International journal of*
17 *molecular sciences*, 24(12), 9793. <https://doi.org/10.3390/ijms24129793>
- 18 Tiwari, A., Mamedov, F., Fitzpatrick, D., Gunell, S., Tikkanen, M., & Aro, E. M. (2024). Differential FeS cluster
19 photodamage plays a critical role in regulating excess electron flow through photosystem I. *Nature plants*, 10(10),
20 1592–1603. <https://doi.org/10.1038/s41477-024-01780-2>
- 21 Tran, H. C., Schmitt, V., Lama, S., Wang, C., Launay-Avon, A., Bernfur, K., Sultan, K., Khan, K., Brunaud, V.,
22 Liehrmann, A., Castandet, B., Levander, F., Rasmusson, A. G., Mireau, H., Delannoy, E., & Van Aken, O. (2023).
23 An mTRAN-mRNA interaction mediates mitochondrial translation initiation in plants. *Science*, 381(6661),
24 eadg0995. <https://doi.org/10.1126/science.adg0995>
- 25 Triozzi, P. M., Brunello, L., Novi, G., Ferri, G., Cardarelli, F., Loreti, E., Perales, M., & Perata, P. (2024).
26 Spatiotemporal oxygen dynamics in young leaves reveal cyclic hypoxia in plants. *Molecular plant*, 17(3), 377–
27 394. <https://doi.org/10.1016/j.molp.2024.01.006>
- 28 Umbach, A. L., Fiorani, F., & Siedow, J. N. (2005). Characterization of transformed Arabidopsis with altered
29 alternative oxidase levels and analysis of effects on reactive oxygen species in tissue. *Plant physiology*, 139(4),
30 1806–1820. <https://doi.org/10.1104/pp.105.070763>
- 31 Van Aken, O., Pecenkova, T., van de Cotte, B., De Rycke, R., Eeckhout, D., Fromm, H., De Jaeger, G., Witters, E.,
32 Beemster, G. T., Inzé, D., & Van Breusegem, F. (2007). Mitochondrial type-I prohibitins of Arabidopsis thaliana
33 are required for supporting proficient meristem development. *The Plant journal : for cell and molecular biology*,
34 52(5), 850–864. <https://doi.org/10.1111/j.1365-313X.2007.03276.x>
- 35 Van Aken, O., Ford, E., Lister, R., Huang, S., & Millar, A. H. (2016). Retrograde signalling caused by heritable
36 mitochondrial dysfunction is partially mediated by ANAC017 and improves plant performance. *The Plant*
37 *journal : for cell and molecular biology*, 88(4), 542–558. <https://doi.org/10.1111/tbj.13276>
- 38 van Dongen, J. T., & Licausi, F. (2015). Oxygen sensing and signaling. *Annual review of plant biology*, 66, 345–
39 367. <https://doi.org/10.1146/annurev-arplant-043014-114813>
- 40 Vanlerberghe G. C. (2013). Alternative oxidase: a mitochondrial respiratory pathway to maintain metabolic and
41 signaling homeostasis during abiotic and biotic stress in plants. *International journal of molecular sciences*, 14(4),
42 6805–6847. <https://doi.org/10.3390/ijms14046805>

- 1 Vanlerberghe, G. C., Dahal, K., Alber, N. A., & Chadee, A. (2020). Photosynthesis, respiration and growth: A
2 carbon and energy balancing act for alternative oxidase. *Mitochondrion*, 52, 197–211.
3 <https://doi.org/10.1016/j.mito.2020.04.001>
- 4 van Veen, H., Triozzi, P. M., & Loreti, E. (2025). Metabolic strategies in hypoxic plants. *Plant physiology*, 197(1),
5 kiae564. <https://doi.org/10.1093/plphys/kiae564>
- 6 Vainonen, J. P., Gossens, R., Krasensky-Wrzaczek, J., De Masi, R., Danciu, I., Puukko, T., Battchikova, N., Jonak,
7 C., Wirthmueller, L., Wrzaczek, M., Shapiguzov, A., & Kangasjärvi, J. (2023). Poly(ADP-ribose)-binding protein
8 RCD1 is a plant PARylation reader regulated by Photoregulatory Protein Kinases. *Communications biology*, 6(1),
9 429. <https://doi.org/10.1038/s42003-023-04794-2>
- 10 Vaseghi, M. J., Chibani, K., Telman, W., Liebthal, M. F., Gerken, M., Schnitzer, H., Mueller, S. M., & Dietz, K. J.
11 (2018). The chloroplast 2-cysteine peroxiredoxin functions as thioredoxin oxidase in redox regulation of
12 chloroplast metabolism. *eLife*, 7, e38194. <https://doi.org/10.7554/eLife.38194>
- 13 Vishwakarma, A., Kumari, A., Mur, L. A. J., & Gupta, K. J. (2018). A discrete role for alternative oxidase under
14 hypoxia to increase nitric oxide and drive energy production. *Free radical biology & medicine*, 122, 40–51.
15 <https://doi.org/10.1016/j.freeradbiomed.2018.03.045>
- 16 Wagner, S., Van Aken, O., Elsässer, M., & Schwarzländer, M. (2018). Mitochondrial Energy Signaling and Its
17 Role in the Low-Oxygen Stress Response of Plants. *Plant physiology*, 176(2), 1156–1170.
18 <https://doi.org/10.1104/pp.17.01387>
- 19 Wang, Y., Selinski, J., Mao, C., Zhu, Y., Berkowitz, O., & Whelan, J. (2020). Linking mitochondrial and
20 chloroplast retrograde signalling in plants. *Philosophical transactions of the Royal Society of London. Series B,*
21 *Biological sciences*, 375(1801), 20190410. <https://doi.org/10.1098/rstb.2019.0410>
- 22 Waszczak, C., Carmody, M., & Kangasjärvi, J. (2018). Reactive Oxygen Species in Plant Signaling. *Annual*
23 *review of plant biology*, 69, 209–236. <https://doi.org/10.1146/annurev-arplant-042817-040322>
- 24 Weits, D. A., van Dongen, J. T., & Licausi, F. (2021). Molecular oxygen as a signaling component in plant
25 development. *The New phytologist*, 229(1), 24–35. <https://doi.org/10.1111/nph.16424>
- 26 Wirthmueller, L., Asai, S., Rallapalli, G., Sklenar, J., Fabro, G., Kim, D. S., Lintermann, R., Jaspers, P., Wrzaczek,
27 M., Kangasjärvi, J., MacLean, D., Menke, F. L. H., Banfield, M. J., & Jones, J. D. G. (2018). Arabidopsis downy
28 mildew effector HaRxL106 suppresses plant immunity by binding to RADICAL-INDUCED CELL DEATH1. *The*
29 *New phytologist*, 220(1), 232–248. <https://doi.org/10.1111/nph.15277>
- 30 Xu, S., Guerra, D., Lee, U., & Vierling, E. (2013). S-nitrosoglutathione reductases are low-copy number, cysteine-
31 rich proteins in plants that control multiple developmental and defense responses in Arabidopsis. *Frontiers in plant*
32 *science*, 4, 430. <https://doi.org/10.3389/fpls.2013.00430>
- 33 Yoshida, K., Noguchi, K. (2011). Interaction Between Chloroplasts and Mitochondria: Activity, Function, and
34 Regulation of the Mitochondrial Respiratory System during Photosynthesis. In: Kempken, F. (eds) *Plant*
35 *Mitochondria. Advances in Plant Biology*, vol 1. Springer, New York, NY. https://doi.org/10.1007/978-0-387-89781-3_15
- 36
- 37 Yoshida, K., Hara, A., Sugiura, K., Fukaya, Y., & Hisabori, T. (2018). Thioredoxin-like2/2-Cys peroxiredoxin
38 redox cascade supports oxidative thiol modulation in chloroplasts. *Proceedings of the National Academy of*
39 *Sciences of the United States of America*, 115(35), E8296–E8304. <https://doi.org/10.1073/pnas.1808284115>
- 40 Zhang, R., Kuo, R., Coulter, M., Calixto, C. P. G., Entizne, J. C., Guo, W., Marquez, Y., Milne, L., Riegler, S.,
41 Matsui, A., Tanaka, M., Harvey, S., Gao, Y., Wießner-Kroh, T., Paniagua, A., Crespi, M., Denby, K., Hur, A. B.,
42 Huq, E., Jantsch, M., ... Brown, J. W. S. (2022). A high-resolution single-molecule sequencing-based Arabidopsis

1 transcriptome using novel methods of Iso-seq analysis. Genome biology, 23(1), 149.
2 <https://doi.org/10.1186/s13059-022-02711-0>

3



4

5

6

7

Figure 1
134x111 mm (x DPI)

ACCEPTED MANUSCRIPT

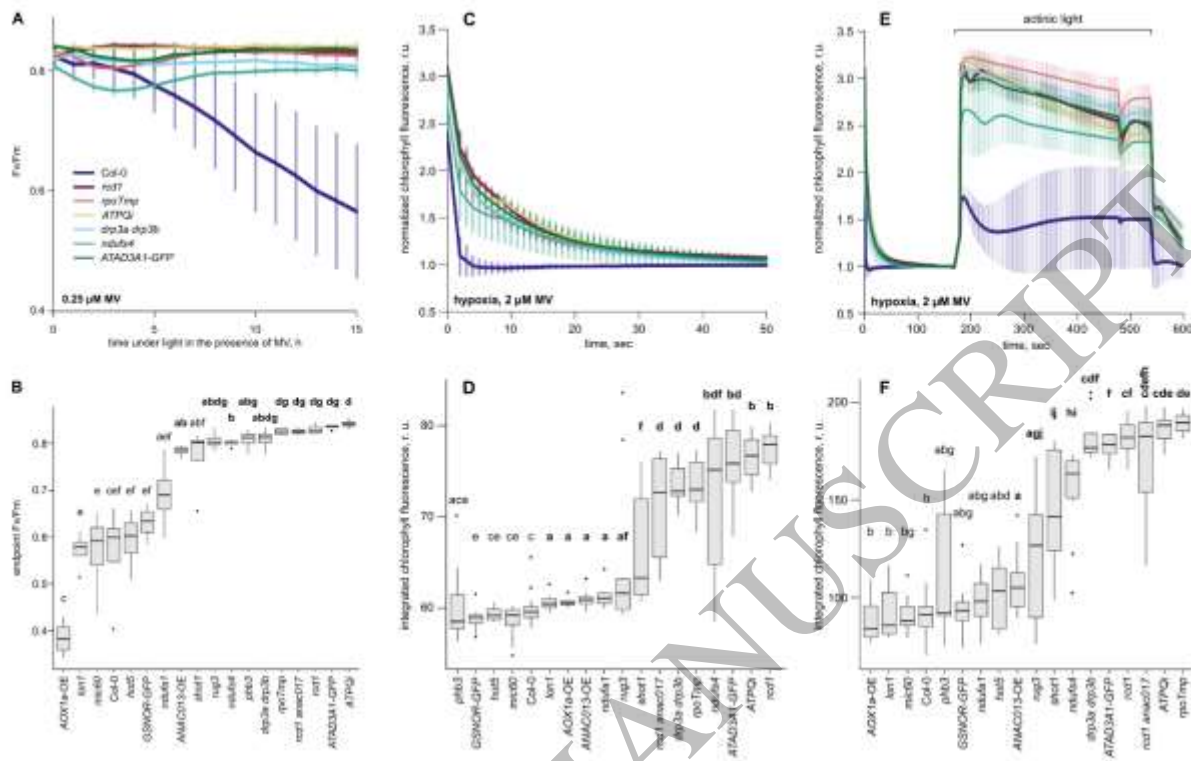


Figure 2
326x211 mm (x DPI)

1
2
3
4

ACCEPTED MANUSCRIPT

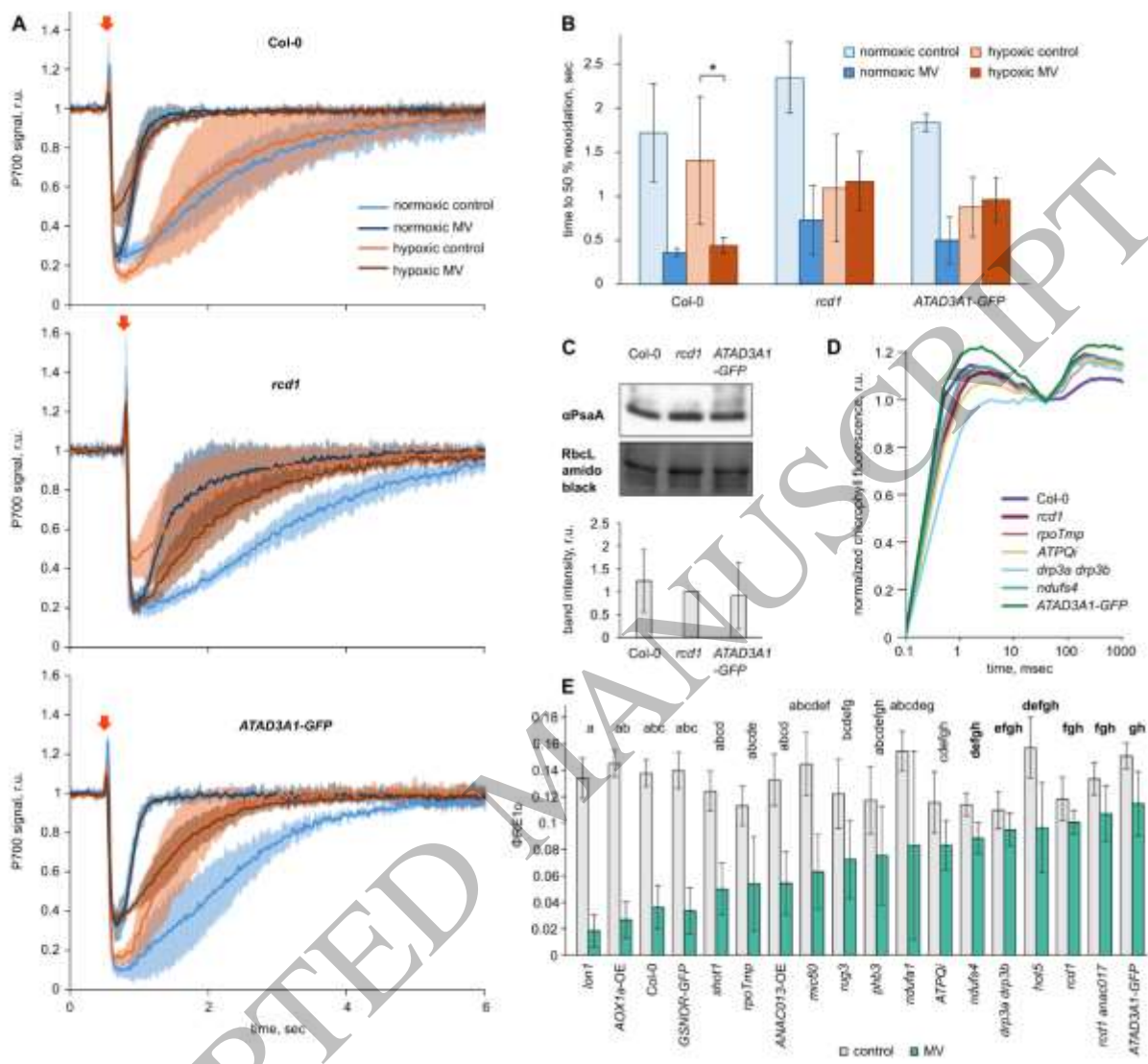


Figure 3
249x231 mm (x DPI)

1
2
3
4

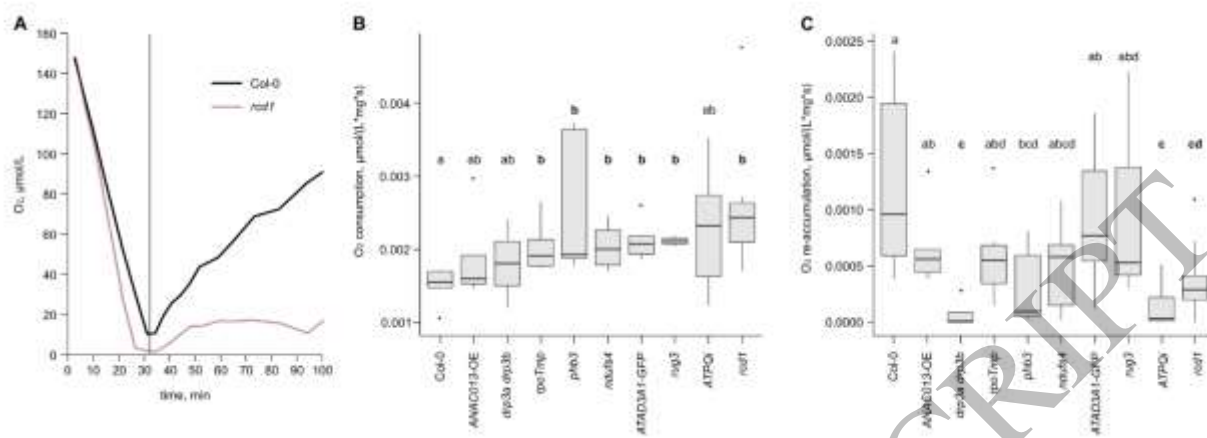


Figure 4
288x108 mm (x DPI)

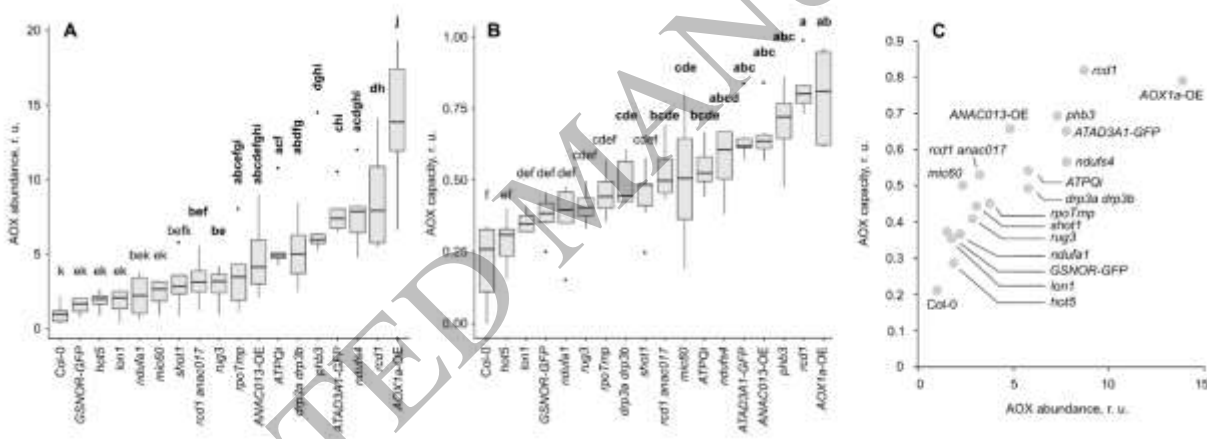


Figure 5
275x105 mm (x DPI)

1
2
3
4

5
6
7
8

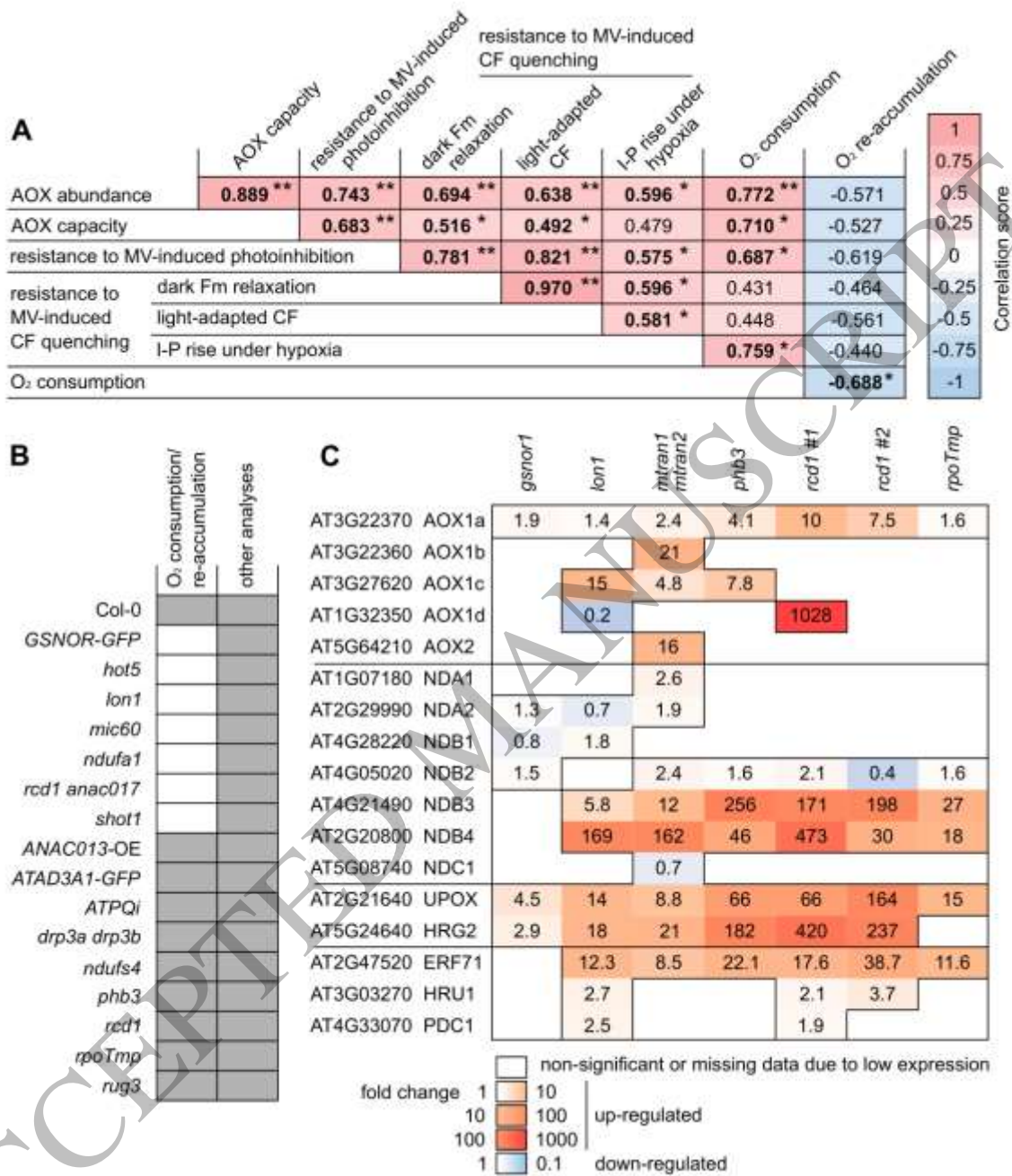


Figure 6
158x179 mm (x DPI)

1
2
3